

UC Davis

UC Davis Electronic Theses and Dissertations

Title

Isoform-specific Disruption of the TP73 Gene Reveals a Critical Role for TAp73gamma in Tumorigenesis via Leptin

Permalink

<https://escholarship.org/uc/item/11j724f1>

Author

Kong, Xiangmudong

Publication Date

2022

Peer reviewed|Thesis/dissertation

Isoform-specific Disruption of the *TP73* Gene Reveals a Critical Role for TAp73gamma in Tumorigenesis via Leptin

By

XIANGMUDONG (DANIEL) KONG
DISSERTATION

Submitted in partial satisfaction of the requirements for the degree of

DOCTOR OF PHILOSOPHY

in

Integrative Pathobiology

in the

OFFICE OF GRADUATE STUDIES

of the

UNIVERSITY OF CALIFORNIA

DAVIS

Approved:

Xinbin Chen, Chair

Robert B Rebhun

Luke Wittenburg

Committee in Charge

2022

Abstract

TP73, a member of the p53 family, is expressed as TAp73 and Δ Np73 along with multiple C-terminal isoforms (α - η). Δ Np73 is primarily expressed in neuronal cells and necessary for neuronal development. Interestingly, while TAp73 α is a tumor suppressor and predominantly expressed in normal cells, TAp73 is found to be frequently altered in human cancers, suggesting a role of TAp73 C-terminal isoforms in tumorigenesis. To test this, the TCGA SpliceSeq database was searched and showed that exon 11 (E11) exclusion occurs frequently in several human cancers. We also found that p73 α to p73 γ isoform switch resulting from E11 skipping occurs frequently in human prostate cancers and dog lymphomas. To determine whether p73 α to p73 γ isoform switch plays a role in tumorigenesis, CRISPR technology was used to generate multiple cancer cell lines and a mouse model in that *Trp73* E11 is deleted. Surprisingly, we found that in E11-deficient cells, p73 γ becomes the predominant isoform and exerts oncogenic activities by promoting cell proliferation and migration. In line with this, E11-deficient mice were more prone to obesity and B-cell lymphomas, indicating a unique role of p73 γ in lipid metabolism and tumorigenesis. Additionally, we found that *E11*-deficient mice phenocopies *Trp73*-deficient mice with short lifespan, infertility, and chronic inflammation. Mechanistically, Mechanistically, we showed that Leptin, a pleiotropic adipocytokine involved in energy metabolism and oncogenesis, was highly induced by p73 γ , necessary for p73 γ -mediated oncogenic activity, and associated with p73 α to γ isoform switch in human prostate cancer and dog lymphoma. Finally, we showed that E11-knockout promoted, whereas knockdown of p73 γ or Leptin suppressed, xenograft growth in mice. Our study indicates that the p73 γ -Leptin pathway promotes tumorigenesis and alters lipid metabolism, which may be targeted for cancer management.

**Isoform-specific Disruption of the *TP73* Gene Reveals a Critical Role for TAp73gamma in
Tumorigenesis via Leptin**

Xiangmudong Kong¹, Wensheng Yan², Wenqiang Sun¹, Yanhong Zhang¹, Hee Jung Yang³,
Mingyi Chen⁴, Hongwu Chen⁵, Ralph W. de Vere White⁶, Jin Zhang^{1,7}, and Xinbin Chen^{1,7}

¹ Comparative Oncology Laboratory, Schools of Veterinary Medicine and Medicine, University of California at Davis, Davis, CA, 95616

² Current address: Berkeley Regional Lab, Pathology/Lab-Histology Department, The Permanente Medical group, Berkeley, CA, 94085

³ Current address: Pharmacology Team, Drug Discovery Center, LG Life Science R&D, LG Chem Ltd, Seoul, Korea. 150-721

⁴ Department of Pathology, University of Texas Southwestern Medical Center, Dallas, TX, 75390

⁵ Department of Biochemistry and Molecular Medicine, University of California at Davis, Davis, CA, 95616

⁶ Department of Urology Surgery, School of Medicine, University of California at Davis, Davis, CA, 95616

⁷ Co-Corresponding Authors

Jin Zhang at jinzhang@ucdavis.edu

Xinbin Chen at xbchen@ucdavis.edu

Running title: TAp73gamma promotes oncogenesis via Leptin

Key words: TAp73, p53, p73 C-terminal isoforms, TAp73gamma, Leptin, oncogenesis, Obesity

Introduction

The *TP73* gene encodes a member of the p53 family of transcription factors involved in tumor suppression and development. *TP73* gene is mapped to a region on chromosome 1p36 that is frequently deleted in neuroblastoma and other tumors, thus linking its role to cancer (1). p73 shares a high similarity with p53 in the transactivation, tetramerization, and DNA binding domains, with most considerable homology between their DNA binding domains (2). Consequently, p73 activates a number of putative p53 target genes involving in cell cycle arrest, apoptosis, and differentiation (2, 3). Despite these similarities, p73 is not functionally redundant to p53. *TP73* is rarely mutated but frequently found to be up-regulated in human cancers, indicating that p73 is not a classic Knudson-type tumor suppressor (4-6). Indeed, the biological functions of p73 have been linked to neurological development, tumorigenesis, ciliogenesis, fertility, and metabolism as illustrated by *in vitro* and *in vivo* models (7-15).

The role of p73 in cancer is complicated due to the presence of multiple p73 isoforms that coordinate in a complex way to exert both oncogenic and non-oncogenic activities (15-19). Through the usage of two promoters, *TP73* encodes two classes of isoforms, TAp73 and N-terminally truncated Δ Np73. TAp73 isoforms, driven by the P1 promoter located upstream of exon 1, contain a transactivation domain similar to that in p53 and thus are suggested to function as a tumor suppressor. Δ Np73 isoforms, arising from the P2 promoter located in intron 3, lack the N-terminal transactivation domain and thus, are thought to have oncogenic potential by acting as dominant-negative inhibitors of p53 and TAp73. Mice deficient in Δ Np73 isoforms are not prone to tumors, but have defects in neurological development similar to that in total p73-KO mice (10, 11). By contrast, mice deficient in TAp73 isoforms develop spontaneous and carcinogens-induced tumors (12), suggesting a role of TAp73 as tumor suppressor. However,

several recent studies also showed that TAp73 exhibits both pro-tumorigenic activities depend on the context (15, 20, 21), suggesting that the role of TAp73 in tumorigenesis is far more complex, likely being affected by the various C-terminal TAp73 isoforms.

At the C-terminus, multiple p73 isoforms are generated due to alternative splicing from exon 11 to 13 (22, 23). At transcript levels, six splicing variants (α , β , γ , δ , ϵ , ζ) can be detected. However, at protein levels, only three isoforms (α , β , and γ) can be detected with α being the most abundantly expressed. Due to lack of proper model systems and reagents, most studies about p73 C-terminal isoforms have been done in cell culture and thus, may not reflect the authentic biological role of these isoforms. When over-expressed, p73 β showed very strong, whereas p73 α and p73 γ exhibited much weaker, activity to induce programmed cell death (24, 25). These differential activities are suggested due to the variation of C-terminal sequence among p73 C-terminal isoforms (23). p73 α , the longest isoform, contains a sterile alpha motif (SAM) and an extreme C-terminal domain, both of which are thought to inhibit its transcriptional activity through interaction with other factors (26). Similarly, p73 γ contains a unique C-terminal domain with unknown function. By contrast, p73 β does not contain an extended C-terminal domain present in both p73 α and p73 γ . Nevertheless, these hypotheses have never been tested *in vivo*. The difficulties to study the physiological roles of p73 C-terminal isoforms are mainly due to the following reasons :1) the presence of TA/ Δ N isoforms with opposing functions, which adds complications to study the C-terminal isoforms; 2) p73 α is the major isoform expressed in most cells and tissues and may shield activities by other isoforms; 3) lack of specific antibodies to detect β or γ isoforms. These limitations may have led to two opposing functions for TAp73 as a tumor suppressor and a tumor promoter (27).

Leptin is a 167-amino-acid peptide hormone encoded by the *Ob* gene and produced by a multitude of tissues, especially adipose tissue (28). Leptin communicates with its receptor (LepR) in the hypothalamus and controls energy expenditure and appetite through a negative feedback loop, thereby maintaining the relative constancy of adipose tissue mass from being too thin or too obese (29, 30). The anti-obesity effect of Leptin was demonstrated in individuals bearing congenital leptin deficiencies (31). It was later found out that leptin therapy is ineffective as most obese individuals have a high level of endogenous plasma leptin (hyperleptinaemia) and do not respond to leptin therapy, a condition called leptin resistance (32). As a pleiotropic cytokine, leptin plays a critical role in lipid/glucose homeostasis, immune responses, hematopoiesis, angiogenesis, reproduction, and mental processes (33-36). Leptin signaling is also found to promote cancer progression, including cell proliferation, metastasis, angiogenesis and chemoresistance (37, 38). Notably, both leptin and LepR are frequently altered in many obesity-associated cancers, including lung, breast, ovarian, pancreas, liver and prostate (39-41). Thus, targeting Leptin-LepR signaling may represent a novel strategy for cancer therapeutics.

To understand the role of various p73 C-terminal isoforms in cancer development, we searched the TCGA SpliceSeq database and found that *Trp73* E11 skipping, which led to isoform switch from p73 α to p73 γ , frequently occurs in a subset of human cancers and dog lymphomas. Thus, to explore the biological function of p73 γ isoform, we employed CRISPR technology to manipulate p73 splicing by deleting E11 in the *TP73* gene in multiple cancer cell lines and mice. We showed that E11-deficiency resulted in p73 γ become the predominant isoform in both human and mouse cells. Unexpectedly, we found that p73 γ , when expressed at a physiologically relevant level, did not behave as a tumor suppressor, but promoted cell migration and

tumorigenesis in vitro and in vivo. Mechanistically, we showed that Leptin, a pleiotropic adipocytokine, was induced by p73 γ and contributes to p73 γ -mediated tumorigenesis. Moreover, we found that p73 α to γ isoform switch was detected in a subset of dog lymphomas and human prostate carcinomas along with elevated expression of Leptin. Finally, we showed that targeting p73 γ or Leptin led to growth suppression of E11-KO xenografts in a mouse xenograft model, suggesting that the p73 γ -Leptin pathway may be explored for cancer management.

Materials and Methods

Reagents

Anti-Actin (sc-47778, 1:3000), anti-p130 (sc-374521, 1:3000), anti-p21 (sc-53870, 1:3000), anti-p130 (sc-374521, 1:3000) and anti-PML (sc-377390, 1:3000) were purchased from Santa Cruz Biotechnology. Anti-TAp73 (A300-126A, 1:2000) was purchased from Bethyl Laboratories. Anti-HA (MMS-101P, 1:3000) was purchased from Covance. Anti-Ki-67 (Cat#12202, 1:100), anti-B220 (Cat#70265, 1:100) and Anti-Leptin (Cat#16227, 1:500) were purchased from Cell signaling. Anti-p73 γ/ϵ antibody was generated by Cocalico Biologicals using a peptide (PRDAQQPWPRSASQRRDEC). To-Pro-3 was purchased from Invitrogen. The WesternBright ECL HRP substrate (Cat# K12043-D20) was purchased from Advansta. Matrigel was obtained from Corning Inc. (Cat# 354230). IHC kit (Cat# PK6100) and DAB (Cat# SK4100) were purchased from Vector laboratories. Dual-Luciferase® Reporter Assay kit was purchased from Promega (Cat# E1910). Scrambled siRNA (5'- GGC CGA UUG UCA AAU AAU U -3'), p73 α/γ siRNA#1 (5'- AGC CUC GUC AGU UUU UUA A -3'), p73 α/γ siRNA#2 (5'- AAC CUG ACC AUU GAG GAC CUG GG -3'), Leptin siRNA#1 (5'- GCU GGA AGC ACA UGU UUA U -3'), and Leptin siRNA#2 (5'- CCA GAA ACG UGA UCC AAA UUU -3') were purchased from Dharmacon (Chicago, IL). For siRNA transfection, RNAiMax (Life Technologies) was used according to the user's manual. Proteinase inhibitor cocktail was purchased from Sigma-Aldrich. Magnetic Protein A/G beads were purchased from MedChem. RiboLock RNase Inhibitor and Revert Aid First Strand cDNA Synthesis Kit were purchased from Thermo Fisher. Recombinant Human Leptin Protein was purchased from R&D (398-LP).

Plasmids

To generate a vector expressing a single guide RNA (sgRNA) that targets total p73, TAp73, Δ Np73 and E11, two 25-nt oligos were annealed and then cloned into the pSpCas9(BB) sgRNA expression vector via BbsI site (42). To generate the pSpCas9(BB)- Δ Np73-sgRNA-Blast vector expressing both blasticidin and Δ Np73 sgRNA, the blasticidin gene was amplified from pcDNA6 vector and then cloned into pSpCas9(BB)- Δ Np73 via NotI. To generate a luciferase reporter that contains the WT Leptin promoter, a DNA fragment was amplified from genomic DNA from H1299 cells, cloned into pGL2-basic vector via XmaI and HindIII sites, followed by sequence confirmation. To generate a luciferase reporter that contains mutant Leptin promoter, two-step PCR was used. The first step was to amplify two DNA fragments (Fragment #1 and #2) by using the WT Lep promoter as the template. Fragment #1 was amplified using WT forward 1 primer and mutant reverse mutant 1 primer. Fragment #2 was amplified using mutant forward 1 primer and WT reverse 1 primer. The second round of PCR was performed by using both fragment #1 and #2 as templates with a WT forward 1 and a reverse 1 primer. The resulted DNA fragment was then cloned into pGL2-basic vector via XmaI and HindIII sites. To generate a pcDNA4 vector expressing HA-tagged TAp73 γ , a 680 bp DNA fragment was amplified by using cDNAs from H1299 cells as a template, and then used to replace the C-terminal of HA-TAp73 α (24) via EcoRI and XhoI sites. The sequences of all primers were listed in Supplemental Table S4.

Mice and MEF isolation

Trp73^{+/-} mice were generated as described previously (43). *E11*^{+/-} mice were generated by the Mouse Biology Program at University of California at Davis. All animals and use protocols were approved by the University of California at Davis Institutional Animal Care and

Use Committee. To generate WT and *E11*^{-/-} MEFs, *E11*^{+/-} mice were bred with *E11*^{+/-} and MEFs were isolated from 12.5 to 13.5 postcoitum (p.c.) mouse embryos as described previously (44). MEFs were cultured in DMEM supplemented with 10% FBS (Life Science Technology), 55 μM β-mercaptoethanol, and 1× non-essential amino acids (NEAA) solution (Cellgro). All the genotyping primers were listed in Supplemental Table S5.

Cell culture, Cell Line Generation

H1299 and Mia-PaCa2 cells and their derivatives were cultured in DMEM (Dulbecco's modified Eagle's medium, Invitrogen) supplemented with 10% fetal bovine serum (Hyclone). MCF-10A cells were cultured in DMEM:F12 (1:1) supplemented with 5% donor horse serum, 20 ng/ml EGF, 10 μg/ml insulin, 0.5 μg/ml hydrocortisone, and 100 ng/ml cholera toxin. To generate Total p73-, TAp73, ΔNP73, and E11-KO cell lines by CRISPR-Cas9, H1299 or Mia-PaCa2 cells were transfected with pSpCas9(BB)-2A-Puro vector expressing a guide RNA, and then selected with puromycin for 2-3 weeks. To generate ΔN/E11-DKO cells, E11-KO H1299 and Mia-PaCa2 cells were transfected with pSpCas9(BB)-ΔNp73-sgRNA-Blast vector, followed by selection with blasticidin for 2-3 weeks. Individual clone was picked confirmed by sequence analysis or western blot analysis. The primers used for sequencing total p73, TAp73, ΔNp73 and p73 exon 11 are listed in Supplemental Table S5. H1299 cells that inducibly express HA-tagged TAp73γ were generated as previously described (45). Briefly, pcDNA4-HA-TAp73 vector was transfected into H1299 cells in which a tetracycline repressor is expressed by pcDNA6 (46). Individual clone was picked and screened and for TAp73g expression by performing western blot analysis. To induce HA-tagged TAp73γ expression, tetracycline was added to the medium.

Western Blot Analysis

Western blot analysis was performed as previously described (47). Briefly, whole cell lysates were harvested by 2×SDS sample buffer. Proteins were separated in 7-13% SDS-polyacrylamide gel, transferred to a nitrocellulose membrane, probed with indicated antibodies, followed by detection with enhanced chemiluminescence and visualized by VisionWorks®LS software (Analytik Jena).

RNA isolation and RT-PCR

Total RNA was isolated with Trizol reagent as described according to user's manual. cDNA was synthesized with Reverse Transcriptase (Promega, San Luis Obispo, CA) and used for RT-PCR. The PCR program used for amplification was (i) 94°C for 5 minutes, (ii) 94°C for 45 seconds, (iii) 58°C for 45 seconds, (iv) 72°C for 30 seconds, and (v) 72°C for 10 minutes. From steps 2 to 4, the cycle was repeated 22 times for actin and GAPDH, 28-35 times depending on the targets. All primers were used for RT-PCR are listed in Supplemental Table S6.

ChIP Assay

ChIP assay was performed as previously described (48). Briefly, chromatin was cross-linked in 1% formaldehyde in phosphate-buffered saline (PBS). Chromatin lysates were sonicated to yield 200- to 1,000-bp DNA fragments and immunoprecipitated with a control IgG or an antibody against HA or p73 γ . After reverse cross-linking and phenol-chloroform extraction, DNA fragments were purified, followed by PCR to visualize the enriched DNA fragments. The primers used for the ChIP assays were listed Supplemental Table S6.

Luciferase reporter assay

Dual luciferase assay was performed according to the manufacturer's instructions (Promega). Briefly, H1299 cells were plated at 5×10^4 cells in triplicate per well in a 24-well plate and allowed to recover overnight. Cells were then transfected with the following plasmids: (1) 3 ng of pRL-SV40-Renilla; (2) 0.25 ug of a luciferase reporter, and (3) 0.25 ug of empty pcDNA3 vector or a pcDNA3 vector expressing p73 α , β , or γ . The relative fold change of luciferase activity is a product of the luciferase activity induced by p73 α , β , or γ divided by that induced by control vector.

Colony formation assay

For Colony formation assay, cells (600 per well) in a six-well plate were cultured for 15 days. The cell clones were fixed with methanol/glacial acetic acid (7:1) and then stained with 0.1% of crystal violet.

Wound healing assay

2×10^5 cells were seeded in a 6-well plate cells and grown for 24 h. The monolayers were wounded by scraping with a P200 micropipette tip and washed two times with PBS. At indicated time points after scraping, cell monolayers were photographed with phase contrast microscopy. Cell migration was determined by visual assessment of cells migrating into the wound. Wound closure percentage was quantified using Image J plugin, Wound Healing Sizing Tool (49), by comparing the width of the wound between 0 h and indicated time points.

Senescence assay

The senescence assay was performed as described previously (50). Briefly, primary MEFs at passage 5 were seeded at 5×10^4 in a well of 6-well plate for 24 hours. Cells were then washed with $1 \times$ phosphate-buffered saline and fixed with 2% formaldehyde, 0.2% glutaraldehyde for 15 mins at room temperature, and then stained with fresh SA- β -galactosidase staining solution [1 mg/mL 5-bromo-4-chloro-3-indolyl- β -D-galactopyranoside, 40mm citric acid/sodium phosphate (pH 6.0), 5mm potassium ferrocyanide, 5 mm potassium ferricyanide, 150mm NaCl, and 2mm MgCl₂]. The percentage of senescent cells was calculated as SA- β -gal positive cell divided by the total number of cells counted.

Histological Analysis and Immunohistochemistry (IHC)

Mouse tissues were fixed in 10% (wt/vol) neutral buffered formalin, processed, and embedded in paraffin blocks. Tissues blocks were sectioned (6 μ m) and stained with hematoxylin and eosin (H&E). Immunohistochemistry (IHC) analysis was performed using the Vectastain ABC Elite Kit (Vector Laboratories) according to manufacturer's instruction. Briefly, tissue sections (5 μ m) were dewaxed and antigen-retrieved in a citrate buffer (pH 6.0), followed by incubation with a primary antibody Anti-Ki-67 (Cat#12202, 1:100), anti-B220 (Cat#70265, 1:100) or Anti-Leptin (Cat#16227, 1:500) overnight at 4 °C and then a secondary antibody for 1 h at room temperature. The slides were visualized by treatment with 3,3'-diaminobenzidine tetrahydrochloride (DAB), and then counterstained with Mayer's hematoxylin.

ELISA

Leptin Elisa was performed using the BioVendor Mouse and Rat Leptin Elisa kit (Cat# RD291001200R). Briefly, mouse serum was incubated with a microplate precoated with mouse leptin antibody. Bound leptin was detected with biotin labelled polyclonal anti-mouse leptin antibody conjugated to horseradish peroxidase and quantified by a chromogenic substrate at 450 nm. A standard curve is constructed by plotting absorbance values versus leptin concentrations of standards, and concentrations of unknown samples are determined using this standard curve. To measure the level of cholesterol and triglycerides, Cholesterol/Cholesterol Ester-Glo™ Assay kit (Cat#J3190, Promega) and Triglyceride-Glo™ Assay kit (Cat#J3160, Promega) from Promega were used according to user's manual. Briefly, mouse sera or cell lysates were first incubated with cholesterol/triglycerides lysis solution at 37°C for 30 min, then incubated with cholesterol/triglycerides detection reagent for 1 hour, followed by luminescence detection with Luminometer (SpectraMAX). A standard curve is constructed and concentrations of unknown samples are determined using the standard curve.

Three-dimensional culture for acini

The assay was performed as previously described (51). Briefly, single cell suspensions were plated onto Matrigel-coated chamber slides at 5000 cells/well in complete growth medium with 2% Matrigel and allowed to grow for 1–22 days. Overlay medium containing 2% Matrigel was renewed every 4 days. At the end of culture, cells were fixed and the nuclei were stained with 5 µg/ml of To-Pro-3 in PBS for 15 min at room temperature. Confocal microscopic images of the acinus structures were captured by the Z-stacking function for serial confocal sectioning at 2-µm intervals (LSM-510 Carl Zeiss laser scanning microscope) and then analyzed by Carl Zeiss software.

Three-dimensional tumor spheroid culture

Single cell suspensions (3,000 cells/well) were plated around the rim of the well of a 96-well plate in a 4:3 mixture of Matrigel and MammoCult medium (BD Bioscience CB-40324). The cell mixture was then incubated at 37°C with 5% CO₂ for 15 min to solidify the gel, followed by addition of 100 µL of pre-warmed MammoCult. At the end of 3-D culture, cells were released from the Matrigel by incubating with 50 µL of dispase (5 mg/mL) (Life Technologies #17105-041) at 37°C for 45 min. Spheroids were imaged by a phase contrast microscope and cell viability was measured by CellTiter-Glo according to manufacturer's guidelines (Promega).

Transwell Migration Assay

Transwell migration assay was performed as previously described (52). Briefly, 1 x 10⁵ cells were seeded in 100 µl of serum free medium in the upper chamber of a 24-well transwell and then incubated at 37°C for 10 minutes to allow cells to settle down. Next, 600 µl of the DMEM with 10% FBS were added to the lower chamber in a 24-well transwell and cells were cultured at 37°C for various time. At the end of each time point, the transwell insert was removed from the plate and cells that had not migrated were removed by a cotton-tipped applicator. Cells that migrated to the other side of membrane were fixed with 70% ethanol for 20 minutes, stained with 0.1% of crystal violet, and photographed by phase contrast microscope. For siRNA knockdown experiment, isogenic control and E11-KO H1299 cells were transfected with a scrambled siRNA or a siRNA against p73 α/γ or Leptin for 48 hours, and then subjected to transwell assays. For Leptin treatment, recombinant Leptin protein (100 ng/ml) was added to media for ten hours.

Tissue collection

The human normal and prostate cancer specimens were obtained from Dr. Ralph De Vere White's group, with consent from patients who underwent radical prostatectomy. Fresh frozen dog lymph nodes from clinical samples were provided by the University of California at Davis Small Animal Clinic with the owner's permission. Samples were homogenized in Trizol, followed by RNA and protein purification according to the users' manual.

Xenograft assay

6×10^6 cells were mixed with Matrigel (1:1 ratio) in 100 μ l and then injected subcutaneously into 8-week-old BALB/c athymic nude mice (Charles River). When tumors were palpable, tumor growth was monitored for every 2 days for a period of up to 17 days. To knock down p73 γ and Leptin *in vivo*, Accell siRNAs against p73 γ or Leptin were synthesized from Dharmacon, which were then transiently transfected into E11-KO H1299 cells along with a scrambled Accell siRNA at a concentration of 7.5 μ M. Two days post transfection, cells were collected and injected into athymic nude mice, followed by monitoring tumor growth as describe above. Mice bearing xenograft tumors also received one more intratumoral injection of Accell siRNAs (7.5 μ M) at day 9. Tumor volume was calculated according to the standard formula: $V = \text{length} \times \text{width} \times \text{depth} \times 0.5236$ (53). At the endpoint, all animals were sacrificed and the tumors weighed. One half of the tumor was stored at -80°C and the other half will be fixed in formalin and embedded with paraffin. Tumors were sectioned and H&E-stained for histopathology examination. All animals and use protocols were approved by the University of California at Davis Institutional Animal Care and Use Committee.

Statistical analysis

The Log-rank test was used for Kaplan–Meier survival analysis. Fisher’s exact test or two-tailed students’ t test was performed for the statistical analysis as indicated. for the statistical analysis of all ELISA. Values of $p < 0.05$ were considered significant.

Three-dimensional tumorspheroid culture

Single cell suspensions (3,000 cells/well) were plated around the rim of the well of a 96-well plate in a 4:3 mixture of Matrigel and MammoCult medium (BD Bioscience CB-40324). The cell mixture was then incubated at 37°C with 5% CO₂ for 15 min to solidify the gel, followed by addition of 100 µL of pre-warmed MammCult. At the end of 3-D culture, cells were released from the Matrigel by incubating with 50 µL of dispase (5 mg/mL) (Life Technologies #17105-041) at 37°C for 45 min. Spheroids were imaged by a phase contrast microscope and cell viability was measured by CellTiter-Glo according to manufacturer’s guidelines (Promega). Transwell Migration Assay Transwell migration assay was performed as previously described(1). Briefly, 1 x 10⁵ cells were seeded in 100 µl of serum free medium in the upper chamber of a 24-well transwell and then incubated at 37°C for 10 minutes to allow cells to settle down. Next, 600 µl of the DMEM with 10% FBS were added to the lower chamber in a 24-well transwell and cells were cultured at 37°C for various time. At the end of each time point, the transwell insert was removed from the plate and cells that had not migrated were removed by a cotton-tipped applicator. Cells that migrated to the other side of membrane were fixed with 70% ethanol for 20 minutes, stained with 0.1% of crystal violet, and photographed by phase contrast microscope. For siRNA knockdown experiment, isogenic control and E11-KO H1299 cells were transfected

with a scrambled siRNA or a siRNA against p73 α/γ or Leptin for 48 hours, and then subjected to transwell assays. For Leptin treatment, recombinant Leptin protein (100 ng/ml) was added to media for ten hours.

Results

p73 α - γ switch is detected in a subset of human prostate carcinomas and dog lymphomas

Early studies have shown that p73 C-terminal isoforms are dysregulated in breast cancer and leukemia (17, 54). However, it is not clear how p73 C-terminal isoforms are altered and whether these alterations play a role in tumorigenesis. In this regard, we examined the splicing pattern of *TP73* in normal and tumor tissues by using the TCGA SpliceSeq database.

Interestingly, we found that the percentage of exon 11 exclusion was much higher in Lung Squamous Cell Carcinomas (LUSCs) and Head-Neck Squamous Cell Carcinomas (HNSCs) when compared to their respective normal tissues (Fig. 1A-B). We would like to note that exon 11 skipping would lead to production of two p73 isoforms, p73 γ that is switched from p73 α and p73 ϵ that is switched from p73 β . Thus, to determine which p73 isoform is altered in cancer tissues, expression of p73 α , p73 γ , and p73 ϵ transcripts were measured in 5 normal human prostates and 16 prostate carcinomas. We found that p73 α was detectable in 5 normal prostates, undetectable in 12 prostate carcinomas, and unaltered or slightly elevated in 4 prostate carcinomas (Fig. 1C-D). By contrast, p73 γ was highly expressed in prostate carcinomas as compared to that in normal prostates (Fig. 1C-D, compare lanes 1-5 with 6-13). Additionally, p73 ϵ was almost undetectable at both normal and prostate cancer tissues (Data not shown). Similarly, we found that p73 α was expressed in 3 normal dog lymph nodes but undetectable in 16 dog lymphomas (Fig. 1E, p73 α panel, compare lanes 1-3 with 4-16). By contrast, p73 γ expression was very low in 3 normal dog lymph nodes but elevated in all 16 dog lymphomas (Fig. 1E, p73 γ panel, compare lanes 1-3 with 4-16). These data suggest that p73 α isoform in normal tissues is switched to p73 γ isoform in cancer tissues and that p73 γ is associated with tumorigenesis.

Deletion of Exon 11 in the *TP73* gene leads to isoform switch from α to γ , resulting in enhanced cell proliferation and migration as well as altered epithelial morphogenesis

To mimic E11 skipping in human cancer tissue and understand the biological functions of p73 γ , CRISPR-Cas9 technology was used to generate stable H1299 and Mia-PaCa2 cell lines in that the splicing acceptor for *TP73* Exon 11 (E11) was deleted by using two guide RNAs (supplemental Fig. 1A). Sequence analysis verified that E11-KO H1299 and Mia-PaCa2 cells contained a deletion of 21-nt in intron 10 and 26-nt in E11 in the *TP73* gene. We predicted that deletion of E11 splicing acceptor would trigger E11 skipping and subsequently, result in C-terminal isoform switching (Fig. 2A). Indeed, we found that when compared to isogenic control cells, E11-KO cells expressed no α/β isoforms, increased levels of γ/ϵ isoforms, and unaltered δ/ζ isoforms (Fig. 2B). Additionally, TA/ Δ Np73 isoforms were expressed at similar levels in both isogenic control and E11-KO H1299 cells (Fig. 2B, TA/ Δ Np73 panels). The isoform switch in E11-KO cells was also confirmed with specific primers that amplify α/γ or β/ϵ isoforms (Supplemental Fig. 1B-C).

Due to lack of specific antibodies and relative low abundance, p73 γ is almost undetectable under normal conditions. Thus, a peptide (PRDAQQPWPRSASQRRDE) derived from the unique C-terminal region in p73 γ/ϵ was used to generate an antibody, called anti-p73 γ/ϵ antibody, which was found to recognize p73 γ/ϵ but not p73 α (Supplemental Fig. 1D). We showed that in isogenic control cells, TAp73 α was the mostly abundant protein expressed as detected by an anti-TAp73 antibody, whereas in E11-KO cells, TAp73 γ became the predominantly expressed isoform and was detected by anti-p73 γ/ϵ antibody under normal and DNA-damage induced conditions (Fig. 2C and Supplemental Fig. 1E). Nevertheless, other p73 isoforms, including p73 β and p73 ϵ , remained undetectable likely due to their low abundance.

These data confirmed that deletion of the acceptor site for E11 in *TP73* led to E11 skipping and subsequently, resulted in isoform switch from p73 α in isogenic control cells to p73 γ in E11-KO cells.

By using two different promoters, p73 C-terminal isoforms are expressed as TA/ Δ Np73 proteins, which are known to have opposing functions (17). Thus, when studying the p73 C-terminal isoforms, it is also important to consider the N-terminal variations. To this end, stable TAp73- or Δ Np73-KO H1299 and Mia-PaCa2 cell were generated (Fig. 2D and Supplemental Fig. 1F) and used as controls to study the function of E11 deficiency. We found that knockout of TAp73 enhanced, whereas knockout of Δ Np73 reduced, colony formation as compared to isogenic control cells (Fig. 2E), consistent with previous reports (55, 56). Interestingly, the number of colonies formed by E11-KO cells was higher than that by TAp73-KO cells, becoming the highest among all four cell lines (Fig. 2E). To verify this, tumor sphere formation assay was performed and showed that loss of TAp73 or E11 promoted, whereas loss of Δ Np73 inhibited, cell proliferation in H1299 cells (Supplemental Fig. 1G). Moreover, to examine whether E11 deficiency affects cell migration, scratch assay was performed. We found that knockout of TAp73 promoted, whereas knockout of Δ Np73 slightly inhibited, cell migration in H1299 and Mia-PaCa2 cells in a time-dependent manner (Fig. 2F and Supplemental Fig. 1H), consistent with previous observations (56, 57). Notably, E11-KO cells migrated even faster than isogenic control or TAp73-KO H1299 and Mia-PaCa2 cells (Fig. 2F and supplemental Fig. 1H). Consistently, transwell migration assay showed that E11-KO H1299 cells exhibited a markedly enhanced ability to transmigrate through a membrane when compared to isogenic control, TAp73-KO, and Δ Np73-KO H1299 cells (Supplemental Fig. 1I). Furthermore, to determine whether E11 deficiency has an effect on epithelial morphogenesis, E11-KO, TAp73-KO and

$\Delta Np73$ -KO MCF10A cells were generated (Supplemental Fig. 1J) and then subjected to three-dimensional (3-D) culture. We found that parental and isogenic control MCF10A cells underwent normal cell morphogenesis (acini with hollow lumen) (Fig. 2G, left two panels) whereas $\Delta Np73$ -KO showed delayed acinus formation (small acini) (Fig. 2G, $\Delta Np73$ panel). Interestingly, E11-KO and TAp73-KO showed aberrant cell morphogenesis (irregular acini with filled lumen) (Fig. 2G, TAp73^{-/-} and E11-KO panels). These data suggest that loss of E11 promotes oncogenesis by altering epithelial cell morphogenesis and enhancing cell proliferation and migration.

TAp73 γ is primarily responsible for the oncogenic effects observed in E11-KO cells

The enhanced potential of cell proliferation and migration in E11-KO cells could be mediated by increased TAp73 γ expression or simply by loss of TAp73 α as similar phenotypes were also observed in TAp73-KO cells albeit to a less extent (Fig. 2E-G and Supplemental Fig. 1G-I). Thus, to characterize the role of TAp73 γ in oncogenesis, stable H1299 cell lines in that TAp73 γ can be inducibly expressed under the control of a tetracycline-inducible promoter were generated (Supplemental Fig. 2A). We showed that upon induction, TAp73 γ promoted cell migration (Supplemental Fig. 2B), consistent with the data from E11-KO cells (Fig. 2F and Supplemental Fig. 1G-I). Next, to determine the role of endogenous p73 γ in cell proliferation and migration, two p73 α/γ siRNAs (si-p73 α/γ #1 or #2), which were designed to target the junction region of E12-E13 or E13-E14 in p73 α/γ mRNA (Supplemental Fig. 3A), were synthesized and found to efficiently knock down p73 α and p73 γ in isogenic control and E11-KO cells (Fig. 3A-B). Next, cell migration was measured by Scratch and Transwell assays. We showed that knockdown of p73 α/γ enhanced cell migration in isogenic control cells (Fig. 3C and

Supplemental Fig. 3B). By contrast, knockdown of p73 α/γ decreased cell migration in E11-KO cells (Fig. 3C and Supplemental Fig. 3B). Similarly, we found that knockdown of p73 α/γ enhanced cell viability of tumor spheres in isogenic control cells but decreased in E11-KO cells (Supplemental Fig. 3C). These data suggested that cell proliferation and migration is inhibited by p73 α , the major isoform in isogenic control cells, but enhanced by p73 γ , the major isoform in E11-KO cells.

p73 γ can be expressed as two isoforms, TAp73 γ and Δ Np73 γ . To determine which p73 γ isoform is responsible for the enhanced cell migration in E11-KO cells, we generated a dual-KO (DKO) cell line by deleting all Δ Np73 isoforms in E11-KO H1299 and Mia-PaCa2 cells. We showed that Δ Np73 transcript was not expressed, whereas a similar amount of TAp73 γ protein was expressed, in Δ Np73/E11-DKO H1299 and Mia-PaCa2 cells as compared to that in E11-KO cells (Fig. 3D-E and Supplemental Fig. 3D-E). We found that the ability of cells to migrate was not altered by Δ Np73/E11-DKO as compared to that by E11-KO (Fig. 3F and Supplemental Fig. 3F). Considering that knockout of Δ Np73 inhibited cell proliferation and migration (Fig. 2E-F and Supplemental Fig. 1G-H), we conclude that TAp73 γ was able to overcome the inhibitory effect of Δ Np73 deficiency on cell proliferation and migration. Together, these data suggest that TAp73 γ is primarily responsible for the enhanced cell proliferation and migration observed in E11-KO cells.

Deletion of E11 in the *Trp73* gene leads to shortened lifespan, increased incidence of spontaneous tumor and chronic inflammation in mice

CRISPR-Cas9 was used to generate a mouse model in that E11 in the *Trp73* gene was deleted (Supplemental Fig. 4A). A cohort of WT, *E11*^{+/+}, and *E11*^{-/-} MEFs was then generated

(Supplemental Fig. 4B) and used to examine whether E11 deficiency would lead to isoform switch in mice. We found that although MEFs mainly expressed p73 α / γ / ζ transcripts, E11 deficiency led to isoform switch from p73 α in WT MEFs to p73 γ in both *E11*^{+/-} and *E11*^{-/-} MEFs (Fig. 4A), which was similar to that in human cells (Fig. 2B). Next, SA- β -gal staining was performed to evaluate whether E11 deficiency had an effect on cellular senescence, an intrinsic mechanism of tumor suppression. Surprisingly, *E11*^{-/-} MEFs were less prone to cellular senescence as compared to WT MEFs (Fig. 4B), along with decreased expression of senescence markers, including PML, p130, and p21 (Fig. 4C).

To examine the biological functions of E11 deficiency *in vivo*, a cohort of *E11*^{+/-} and *E11*^{-/-} mice were generated. We found that *E11*^{-/-} mice were runty, infertile and prone to hydrocephalus (Supplemental Fig. 4C and data not shown). Thus, *E11*^{-/-} mice exhibited similar phenotypes as *Trp73*^{-/-} mice (7, 14) and were not suitable for long-term tumor study. However, young *E11*^{+/-} mice appeared to be normal. In this regard, a cohort of *E11*^{+/-} mice was generated and monitored for potential abnormalities along with WT and *Trp73*^{+/-} mice. We would like to mention that to minimize the number of animals used, all WT and 26 out of 30 *Trp73*^{+/-} mice, which were generated previously but had same genetic background and maintained in the same facility (43, 58, 59), were used as controls. We found that the lifespan for *E11*^{+/-} mice (96 weeks) and *Trp73*^{+/-} mice (88 weeks) was much shorter than that for WT mice (117 weeks) (Fig. 4D). However, there was no difference in lifespan between *Trp73*^{+/-} and *E11*^{+/-} mice (Fig. 4D). Pathological analysis indicated that 11 out of 51 WT mice, 13 out of 27 *Trp73*^{+/-} mice, and 17 out of 28 *E11*^{+/-} mice developed spontaneous tumors (Fig. 4E; Supplemental Tables 1-3). Statistical analysis indicated that the tumor incidence was significantly higher for both *Trp73*^{+/-} and *E11*^{+/-} mice as compared to that for WT mice (p=0.0211 for WT vs. *Trp73*^{+/-}; p=0.0011 for

WT vs. *E11*^{+/-} by Fisher's exact test). Interestingly, although there was no difference in tumor incidence between *E11*^{+/-} and *Trp73*^{+/-} mice, the percentage of diffuse large B cell lymphoma (DLBCL) was significantly higher in *E11*^{+/-} mice (50%) than that in *Trp73*^{+/-} mice (14.8%) (Fig. 4E and Supplemental Fig. 4D) (p=0.009 by Fisher exact test). These data suggest a role of p73 γ in promoting B-cell lymphomagenesis, which is consistent with the observation that p73 γ is frequently up-regulated in dog lymphomas (Fig. 1E).

In addition to tumors, *E11*^{+/-} mice developed other pathological defects, including chronic inflammation, EMH, and hyperplasia in lymph node, thymus or spleen. Specifically, 17 out of 27 *Trp73*^{+/-} and 8 out of 28 *E11*^{+/-} mice, whereas 0 out of 51 WT mice, showed chronic inflammation in 3 or more organs (Fig. 4F; Supplemental Fig. 4E and Tables 1-3). The chronic inflammation was much less severe in *E11*^{+/-} mice as compared to *Trp73*^{+/-} mice (Fig. 4F), suggesting that p73 γ partially compensates p73 α in suppressing inflammatory response. Moreover, when compared to WT mice, *Trp73*^{+/-} and *E11*^{+/-} mice were prone to EMH (Fig. 4G). Furthermore, *Trp73*^{+/-} and *E11*^{+/-} mice showed various degree of hyperplasia in immune organs, such as lymph node, spleen and thymus when compared to WT mice (Fig. 4H-J). Briefly, the percentage of splenic hyperplasia was higher in *Trp73*^{+/-} and *E11*^{+/-} mice than that in WT mice, with *Trp73*^{+/-} even higher than *E11*^{+/-} mice (Fig. 4H). The percentage of lymphoid hyperplasia was higher in *E11*^{+/-} mice than that in WT and *Trp73*^{+/-} mice (Fig. 4I), whereas the percentage of thymic hyperplasia was higher in *Trp73*^{+/-} mice than that in WT and *E11*^{+/-} mice (Fig. 4J). Together, these data indicated that *E11*-deficient mice phenocopies *Trp73*-deficient mice in short lifespan, infertility, chronic inflammation and tumor incidence, indicating that p73 γ cannot compensate p73 α for tumor suppression and fertility.

***E11*-deficient mice are prone to obesity**

We noticed that *E11*^{+/-} mice were bigger and fatter as compared to WT mice. We also found that the size of adipocytes was larger in both male and female *E11*^{+/-} mice than that in WT mice (Fig. 5A). Likewise, a significant increase in visceral fat (VAT) mass was observed in both male and female *E11*^{+/-} mice as compared to WT mice (Fig. 5B-C). Moreover, when compared to WT mice, *E11*^{+/-} but not *Trp73*^{+/-} mice showed increased incidence in liver steatosis as characterized by lipid deposition in the hepatocytes (Fig. 5D-E). Consistently, the levels of transcripts for alanine aminotransferase (ALT), aspartate aminotransferase (AST), and γ -glutamyltransferase 1 (GGT1) (60, 61), all of which are associated with liver steatosis, were increased in *E11*^{+/-} livers when compared to WT liver (Supplemental Fig. 5A). These observations let us speculate that E11 deficiency promotes obesity in mice. To test this, the level of serum cholesterol and triglycerides was measured and found to be much higher in *E11*^{+/-} mice than that in WT and *Trp73*^{+/-} mice at ~65 weeks (Fig. 5F-G), suggesting that E11 deficiency enhances lipid storage. Consistent with this, younger *E11*^{+/-} mice at 20 or 32 weeks also showed increased body weights (Fig. 5H-I) and elevated levels of serum cholesterol and triglycerides (Fig. 5J-K) when compared to WT mice. Furthermore, to examine whether p73 γ is responsible for decreased lipid catabolism observed in *E11*^{+/-} mice, the level of cholesterol and triglycerides was measured in isogenic control and E11-KO cells with or without knockdown of p73 γ . We found that E11 deficiency led to marked increase in the level of cholesterol and triglycerides in both H1299 and Mia-PaCa2 cells (Fig. 5L-N and Supplemental Fig. 5B-D). However, upon knockdown of p73 γ , elevated level of cholesterol and triglycerides by E11-KO was reduced to normal level in isogenic control cells (Fig. 5L-N and Supplemental Fig. 5B-D). By contrast, the level of cholesterol and triglycerides was increased by knockdown of p73 α/γ in isogenic control H1299 and Mia-PaCa2 cells (Fig. 5L-N and Supplemental Fig. 5B-D), suggesting a role of p73 α

in inhibiting lipid storage. Together, these data suggest that *E11* deficiency leads to obesity in mice, which is largely induced by TAp73 γ .

E11 deficiency leads to elevated production of Leptin, a novel target of TAp73 γ

Several studies have shown that dysfunctional adipose tissues secrete adipocytokines, such as leptin, and subsequently, promote adipose tissue and systemic inflammation, which is considered to be responsible for many obesity-related complications, including cancer (62-64). Interesting, we found that *E11*^{+/-} but not WT mice showed pronounced low-grade inflammation in visceral adipose tissues (VATs) (Supplemental Fig. 6A) as well as increased expression of several proinflammatory cytokines, such as IL6, IL1 α and TNF α , in VAT and liver (Fig. 6A). These observations prompted us to speculate whether E11 deficiency leads to altered expression of leptin, a pleiotropic adipocytokine that is known to be associated with obesity, adipose tissue inflammation and cancer (65-67). In addition to adipocytes, Leptin was found to be expressed in normal epithelial and carcinoma cells and subsequently, promotes tumor growth through autocrine and paracrine signaling (68, 69). Indeed, we found that the level of leptin transcript was increased by E11 deficiency in the VAT and liver tissues as well as in MEFs (Fig. 6A and Supplemental Fig. 6B). Consistent with this, IHC assay showed an elevated expression of leptin protein in *E11*^{+/-} kidney and liver as compared to WT kidney and liver, respectively (Supplemental Fig. 6C). Moreover, the level of Leptin protein in the VAT and serum was highly increased in age- and gender-matched *E11*^{+/-} mice as compared to that in WT and *Trp73*^{+/-} mice (Fig. 6B-C). While Leptin expression was increased in *Trp73*^{+/-} mice, it was still much lower than that in *E11*^{+/-} mice (Fig. 6B-C). Furthermore, the level of serum Leptin was found to be increased in both male and female *E11*^{+/-} mice at very young ages of 20- or 32-week-old when

compare to WT mice (Fig. 6D-E).

The observations above let us speculate whether increased expression of p73 γ in E11-deficient mice contributes to Leptin expression. To test this, Leptin transcript was measured in VATs from age- and gender-matched WT, *Trp73*^{+/-}, and *E11*^{+/-} mice. We found that the level of Leptin transcript was slightly increased in *Trp73*^{+/-} mice, but markedly increased in *E11*^{+/-} mice (Fig. 6F), suggesting that Leptin expression is induced by p73 γ . To verify this, Leptin transcript was measured in TP73-KO, TAp73-KO, Δ Np73-KO, and E11-KO H1299 cells. We found that knockout of all p73 or TAp73 decreased, whereas knockout of Δ Np73 had little effect on, the level of Leptin transcript (Fig. 6G). However, the level of Leptin was much higher in E11-KO cells when compared to isogenic control, TP73-, TAp73-, and Δ Np73-KO H1299 cells (Fig. 6G). We also showed that ectopic expression of TAp73 γ led to increased expression of Leptin (Supplemental Fig. 6D) whereas knockdown of p73 γ markedly decreased the level of Leptin transcript in E11-KO H1299 and Mia-PaCa2 cells (Fig. 6H and Supplemental Fig. 6E). Interestingly, knockdown of p73 α/γ also led to reduction of Leptin expression in isogenic control cells in that p73 α is the predominant isoform (Fig. 6H and Supplemental Fig. 6E), suggesting that p73 α can regulate Leptin transcription. To further test this, we found that ectopic expression of TAp73 α , TAp73 β , or TAp73 γ alone was able to induce Leptin expression, with strongest induction by TAp73 γ (Supplemental Fig. 6F).

To determine whether Leptin is a direct target of TAp73, we searched the Leptin promoter and found a potential p73 response element (p73-RE) located at nt -346 to -321 (Fig. 6I). Thus, ChIP assay was performed and showed that ectopic TAp73 γ was able to bind to the LEP promoter (Fig. 6J). As a positive control, TAp73 γ bound to the p21 promoter (Fig. 6J), a bona fide target of the p53 family (70). Consistent with this, endogenous p73 γ were able to bind

to the Leptin promoter in E11-KO H1299 cells as compared to isogenic control cells (Fig. 6K). Furthermore, to determine whether the p73-RE (nt -346 to -321) is required for TAp73 to transactivate the Leptin promoter, luciferase reporters that contain WT or mutant p73-RE were generated (Fig. 6I). We found that TAp73 $\alpha/\beta/\gamma$ were able to activate the Leptin-WT reporter, with the strongest activation by TAp73 γ (Fig. 6L). By contrast, all TAp73 isoforms were unable to transactivate the luciferase reporter containing mutant p73-RE (Fig. 6L). Together, these data indicate that Leptin is a novel target of TAp73 γ and may play a role in TAp73 γ -induced oncogenic activities.

Leptin is a critical mediator of TAp73 γ in oncogenesis and altered lipid metabolism

Leptin is known to play a critical role in oncogenesis through altered lipid metabolism (71-73). Thus, we examined whether knockdown of Leptin has any effect on the level of cholesterol and triglycerides by using two different Lep siRNAs in both H1299 and Mia-PaCa2 cells (Fig. 7A and Supplemental Fig. 7A). We showed that knockdown of Leptin abrogated the elevated level of cholesterol and triglycerides by E11-KO in both H1299 and Mia-PaCa2 cells (Fig. 7B-C and Supplemental Fig. 7B-C), consistent with the observation that knockdown of p73 γ also abrogated the elevated level of cholesterol and triglycerides by E11-KO (Fig. 5M-N and Supplemental Fig. 5C-D). Next, we examined the role of Leptin in cell migration and showed that in isogenic control cells, cell migration was moderately inhibited by knockdown of Leptin in both H1299 (Fig. 7D-E and Supplemental Fig. 7D) and Mia-PaCa2 cells (Supplemental Fig. 7E-F). By contrast, the enhanced cell migration by E11-KO was abolished by knockdown of Leptin in both H1299 (Fig. 7D-E and Supplemental Fig. 7D) and Mia-PaCa2 cells (Supplemental Fig. 7E-F), consistent with the observation that knockdown of p73 γ also

abolished the enhanced cell migration by E11-KO (Fig. 3C and Supplemental Fig. 3B). To further analyze the role of Leptin in p73 γ -mediated cell migration, we asked whether supplementation of Leptin would have an effect on cell migration. To make sure that the effect of Leptin is transmitted through its receptor, we measure the expression of Leptin receptor (LepR). We found that LepR was expressed at a similar level across isogenic control, TAp73-KO and E11-KO H1299 cells (Supplemental Fig. 7G), suggesting that these cells have an intact Leptin signaling pathway and that LepR expression is not regulated by p73. Importantly, we found that cell transmigration was enhanced by treatment with Leptin in isogenic control, TAp73-KO and E11-KO H1299 cells (Supplemental Fig. 7H). Furthermore, to determine whether the p73 γ -Leptin axis plays a role in cancer progression, we examined whether the expression pattern of Leptin is correlated with that of p73 γ in human prostate carcinomas and dog lymphomas. We found that Leptin expression was low in normal human prostates but highly elevated in prostate carcinomas, which correlates well with the expression of p73 γ (Fig. 7F-G, Leptin and p73 γ panels, compare lanes 1-5 with 6-13). Similarly, Leptin and p73 γ transcripts were found to be highly expressed coordinately in dog lymphomas as compared to normal dog lymph nodes (Fig. 7H, Leptin and p73 γ panels, compare lanes 1-3 with 4-19). These data suggest that Leptin is a mediator of TAp73 γ in oncogenesis and altered lipid metabolism and that the TAp73 γ -Leptin pathway plays a role in the development of prostate cancer and lymphoma.

Targeting p73 γ or Leptin inhibits tumor growth *in vivo*

To explore the therapeutic potential of targeting the p73 γ -Leptin pathway for cancer management, xenograft models were established by using isogenic control and E11-KO H1299 cells. We showed that loss of E11 led to enhanced tumor growth (Fig. 8A). Consistent with this,

tumor size and weight were significantly greater for E11-KO group than that for control group (Fig. 8B-C). We also showed that the levels of p73 γ and Leptin transcripts and proteins were much higher in E11-KO tumors than that in WT tumors (Fig. 8D and supplemental Fig. 8A). Additionally, H.E analysis showed that both WT and E11-KO H1299 xenografts were human cells (Fig. 8E). Next, we determined whether the elevated levels of p73 γ and Leptin are responsible for the enhanced tumor growth by E11-KO. To test this, siRNAs against p73 γ or Leptin were synthesized along with a scrambled siRNA as a control. We found that the rate of growth for E11-KO tumors injected with p73 γ or Leptin siRNA was much slower than the ones injected with the control scrambled siRNA (Fig. 8F). Consistent with this, the tumor size and weight were much less for E11-KO tumors injected with p73 γ or Leptin siRNA than the ones injected with the control scrambled siRNA (Fig. 8G-H). As expected, we showed that both p73 γ and Leptin were efficiently knocked down by their respective siRNAs (Fig. 8I and Supplemental Fig. 8B-C). Notably, we found that treatment with p73 γ or Leptin siRNA led to extensive tumor necrosis in xenografts as compared with that treated with the control scrambled siRNA (Fig. 8J). Together, we showed that E11-KO promotes, whereas knockdown of p73 γ or Leptin suppresses, xenograft growth in mice.

Discussion

The biology of p73 is complicated because p73 is expressed as multiple N- and C-terminal isoforms, some of which may have opposing functions. While TA and Δ Np73 isoforms are shown to exert opposing activities in tumorigenesis by multiple *in vitro* and *in vivo* model systems, the biological significance of C-terminal p73 splicing variants (α , β and γ) remains

largely uncharacterized. In this study, we aimed to manipulate alternative splicing of *TP73* using CRISPR-Cas9. We showed that deletion of E11 in *TP73* leads to isoform switch from p73 α to p73 γ in both human cancer cells and mice. Importantly, we found that owing to p73 γ expression, E11 deficiency leads to enhanced tumorigenesis and obesity *in vitro* and *in vitro*. Moreover, we identified Leptin, a key hormone in energy homeostasis, as a novel target of p73 and a critical mediator of TAp73 γ in oncogenesis and aberrant lipid metabolism. Furthermore, we showed that p73 α - γ switch is detected in a subset of dog lymphomas, along with elevated expression of Leptin. Finally, to explore the therapeutic potential of the p73 γ -Leptin pathway, we showed that E11-KO promotes, whereas knockdown of p73 γ or Leptin suppresses, H1299 xenograft growth in mice. These results have provided compelling evidence and prompted us to hypothesize that p73 C-terminal isoforms, that is, TAp73 α and TAp73 γ , can exert two opposing functions in tumorigenesis in a manner similar to that by TA and Δ N p73 isoforms. These results may have also explained the discrepancies in several early studies that TAp73 have both pro- and anti-tumorigenic activities (15, 19-21, 27, 74-76), which are exerted by TAp73 α and TAp73 γ , respectively. A model to elucidate the role of p73 α / γ switch and the p73 γ -Leptin axis in tumorigenesis is proposed and shown in the Fig. 8J.

We and others have shown that ectopic expression of TAp73 α and TAp73 γ can inhibit cell growth albeit to a much less extent when compared to p53 or TAp73 β (24, 25, 77, 78), suggesting that TAp73 α and TAp73 γ have a role in tumor suppression. Here, we showed that when expressed at a physiological relevant level *in vivo*, TAp73 γ possesses an oncogenic activity whereas TAp73 α has a tumor suppressive function. Specifically, we showed that knockout or knockdown of TAp73 α , the major isoform in H1299 and MiaPaCa2 cells, leads to enhanced cell

proliferation and migration (Figs. 2E-G and 3C, Supplemental Fig. 1G-I). By contrast, *E11* deficiency, which switches TAp73 α to TAp73 γ , leads to enhanced cell proliferation and migration as well as xenograft tumor growth, which can be attenuated by knockdown of p73 γ (Fig. 2E-G, 3C, and 8, Supplemental Fig. 1G-I, 3B-C, and 3F). Moreover, mice deficient in *Trp73*, presumably p73 α , were prone to spontaneous tumors, such as lymphoma (Fig. 4E), consistent with previous observations that loss of *Trp73* promotes Myc-induced B-cell lymphomas or mutant p53-mediated T-cell lymphomas (43, 79). By contrast, *E11*-deficient mice were prone to spontaneous tumors, such as DLBCLs (Fig. 4E and supplemental Table 3), presumably due to elevated p73 γ expression in these mice. Furthermore, we showed that while p73 α was detectable in normal tissues, p73 γ was elevated in a subset of dog lymphomas (Fig. 1C). These data suggest that p73 α and p73 γ have opposing functions in tumorigenesis and that isoform switch from p73 α to p73 γ is a critical event for cancer progression. Indeed, we found that percentage of exon 11 exclusion, which would produce p73 γ isoform, was much higher in tumor samples as compared to normal tissues (Fig. 1A-B). In line with this, TAp73 γ transcript was found to be aberrantly expressed in human hematological malignancies, such as leukemia and non-Hodgkin's lymphomas (80-82). Moreover, one study showed that in breast cancer, p73 α and p73 β are the main isoforms expressed in normal breast tissues whereas other C-terminal splice variants, including p73 γ , are mainly detected in breast cancers (54). Thus, further studies are warranted to examine the expression profile of p73 γ in various types of cancers. Moreover, it is important to identify the splicing factor that regulates the isoform switch from p73 α to p73 γ , which would further our understanding of p73 splicing variants in cancer development.

In addition to tumorigenesis, we noticed that p73 α and p73 γ have distinct and overlapped roles in multiple pathological processes based on the phenotypes from *Trp73*- and *E11*-deficient

mice. We reasoned that if p73 γ can compensate for loss of p73 α , no abnormalities would be observed in *E11*-deficient mice. Instead, we found that both *Trp73*- and *E11*-deficient mice were runty, infertile, and prone to hydrocephalus (Supplemental Fig. 4C and data not shown) (7). We also found that *Trp73*-deficient mice and to a lesser degree, *E11*-deficient mice were susceptible to chronic inflammation and splenic hyperplasia (Fig. 4F and 4H). These data indicate that p73 α has distinct roles in hydrocephalus, fertility, chronic inflammation and splenic hyperplasia, which cannot be fully substituted by p73 γ . On the other hand, p73 γ appeared to have a prominent role in lipid metabolism. Specifically, we found that *E11*-deficient mice were prone to spontaneous liver steatosis, increased body weight and VAT mass, and elevated serum triglycerides and cholesterol, all of which were not observed in *Trp73*-deficient mice (Fig. 5A-E). To verify the role of p73 γ in lipogenesis, we showed that the elevated level of cholesterol and triglycerides by *E11*-KO was abrogated by knockdown of p73 γ (Fig. 5L-N and Supplemental Fig. 5B-D). Together, these data suggest that p73 α and p73 γ may have opposing roles in lipid metabolism in that p73 γ promotes, whereas p73 α inhibits, lipogenesis.

In this study, we found that Leptin expression is induced by p73 γ , leading to elevated level of Leptin in serum, VAT, and possibly many other tissues (Fig. 6A and Supplemental Fig. 6B-C). We also found that accumulation of cholesterol/triglycerides and enhanced cell migration by *E11* deficiency are abrogated by knockdown of Leptin (Fig. 7B-C and 7E; Supplemental Fig. 7B-F), which phenocopies the effect of p73 γ -knockdown in *E11*-KO cells (Fig. 3C and Supplemental Fig. 1G-I and 5C-D). In line with this, we found that Leptin treatment was able to promote cell transmigration in isogenic control, TAp73-KO and *E11*-KO H1299 cells (Supplemental Fig. 7H), indicating that Leptin functions as a mediator of p73 in promoting cell migration. To uncover the mechanism, we showed that Leptin is a target of p73 γ

(Fig. 6F-L). Interestingly, we noticed that while capable, p73 α is much weaker than p73 γ to induce Leptin expression (Fig. 6L and Supplemental Fig. 6F). One possibility is that the unique C-terminal domains in p73 α and p73 γ can recruit distinct sets of transcription coactivators and thus, differentially regulate gene expression, including Leptin, which warrants further investigation.

To explore the physiological significance of the p73 γ -Leptin pathway, we found that Leptin expression correlates well with isoform switch from p73 α to p73 γ in a set of dog lymphomas (Fig. 7F). Leptin was initially found to control energy homeostasis through the hypothalamus and was given a high hope for treating obesity (83). However, it was found later that both too little and too much Leptin can lead to obesity (84, 85), referred to as “leptin resistance” (86, 87). At this moment, it is uncertain whether Leptin directly contributes to obesity mediated by p73 γ , partially due to the above-mentioned paradoxical roles of Leptin in obesity. However, since obesity is now considered a risk factor for many cancers, the p73 γ -Leptin pathway may provide a physiological link between cancer and obesity. Indeed, it should be noted that many studies, including data from this study, indicate that Leptin and its receptor are expressed in both normal and tumor tissues and that Leptin is found to promote inflammation, tumor growth, and angiogenesis (71, 88). Considering that the p73 γ is highly expressed in tumors such as dog lymphoma (Fig. 1C), it is possible that p73 γ plays a critical role in activating the Leptin signaling pathway in tumors, which subsequently promotes tumorigenesis. Moreover, we found that knockdown of p73 γ or Leptin was able to inhibit growth of E11-KO xenograft tumors (Fig. 8), which would open a new revenue for cancer management by targeting the p73 γ -Leptin pathway. Together, these data indicate that as a target

of p73, Leptin mediates p73 γ in tumor promotion and altered lipid metabolism and that the p73 γ -Leptin pathway can be targeted for cancer management.

Conclusion

Our studies indicate that p73 α - γ switch may be a common phenomenon during cancer development and that TAp73 α and TAp73 γ exhibit two opposing functions in tumorigenesis. Our studies also provide compelling evidence that p73 γ has an oncogenic activity and that the p73 γ -Leptin pathway plays a critical role in promoting tumorigenesis and lipid metabolism, which can be explored as a novel cancer treatment strategy by blocking Leptin signaling in p73 γ -expressing tumors.

Abbreviations

E11: exon 11; SAM: Sterile alpha motif; LepR: Leptin Receptor; TCGA: The Cancer Genome Atlas; CRISPR: Clustered regularly interspaced short palindromic repeats; MEF: Mouse Embryonic Fibroblast; KO: knockout; LUSC: Lung squamous cell carcinoma; HNSC: Head-neck squamous cell carcinoma; WT: Wild type; EMH: Extramedullary hematopoiesis; ALT: Alanine aminotransferase; AST: aspartate aminotransferase; GGT1: γ -glutamyltransferase 1; VAT: Visceral adipose tissue; IL6: Interleukin 6; IL1 α : Interleukin 1 α ; TNF α : Tumor necrosis factor α ; IHC: Immunohistochemistry; p73-RE: p73 response element, DLBCL: Diffuse large b cell lymphoma.

Ethical Approval

All animals and use protocols were approved by the University of California at Davis Institutional Animal Care and Use Committee.

Competing interests

The authors declare no competing interests.

Authors' contributions

J.Z., X.C., and X.K. designed the research. X.K., W.Y., W.S., Y.Z., H.J.Y. and J.Z. performed the research. J.Z., M.C., H.C., and X.C. analyzed the data. J.Z., X.C., and X.K. wrote the paper. All authors approved the submitted and final versions of the manuscript.

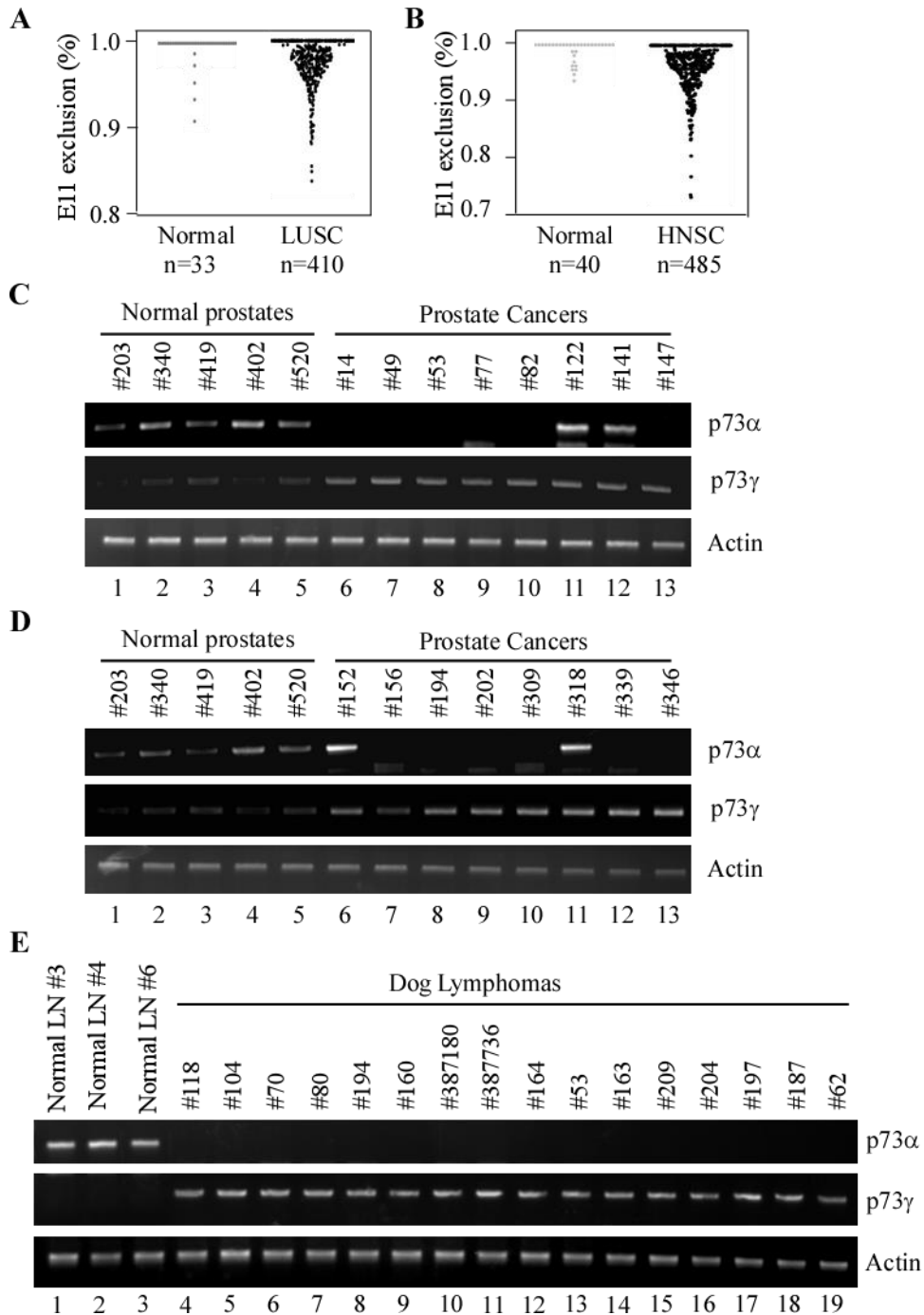
Funding

This work was supported in part by National Institutes of Health R01 grants (CA081237 and CA224433) and UC Davis Cancer Center Core Support Grant CA093373 to X. Chen and by Tobacco-related disease research program (T31IP1727) and the CCAH (Center for Companion Animal Health, UC Davis) grants 2019-13-F and 2021-7-F to J. Zhang.

Availability of data and materials

The authors confirm that the data supporting the findings of this study are available within the article and its supplementary materials.

Figure 1 E11-skipping is detected in a subset of human cancers and dog lymphomas.

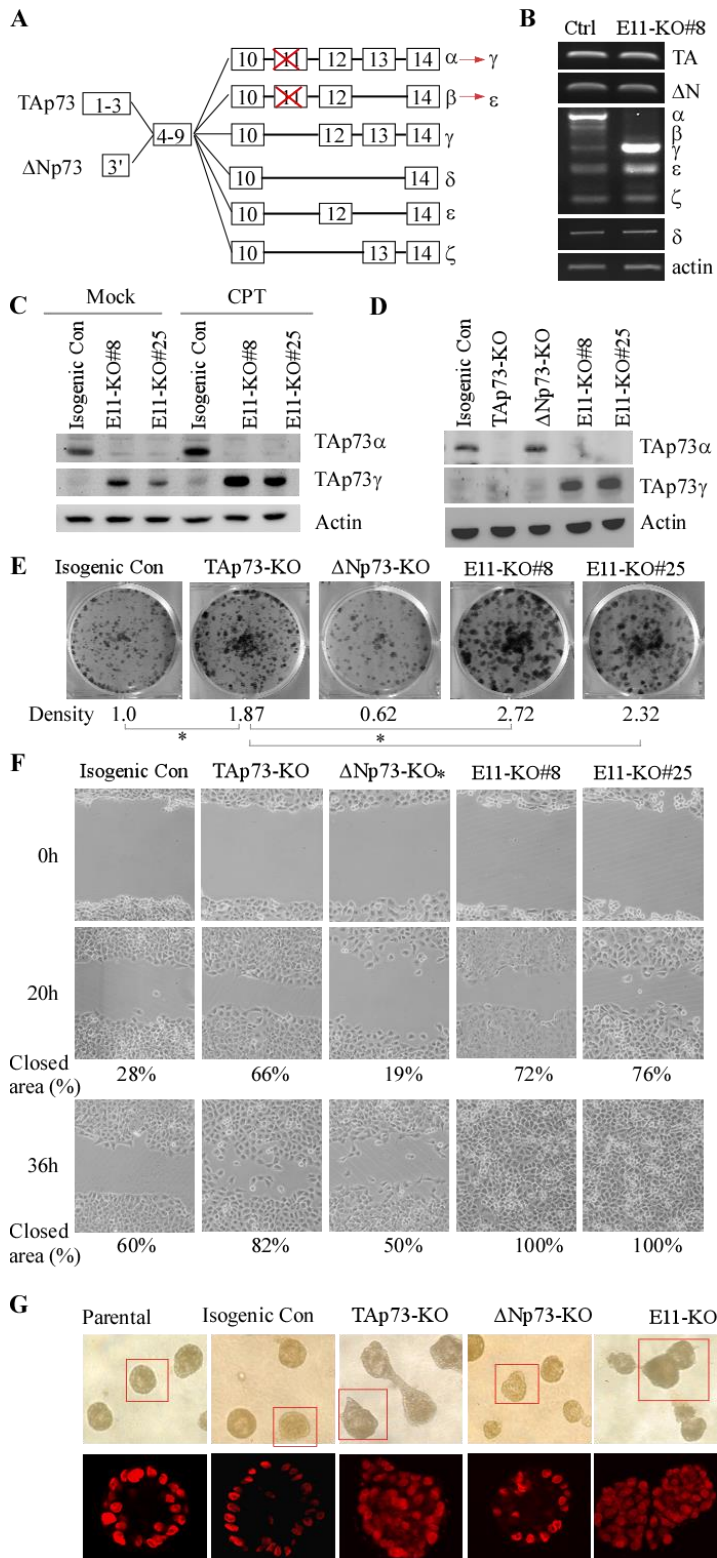


(A-B) Percentage of *TP73* exon 11 exclusion were examined in LUSC (Lung Squamous Cell Carcinoma) and HNSC (Head-Neck Squamous Cell Carcinoma) along with their normal tissues by using TCGA SpliceSeq database. Value of 1 indicates 100% of the transcripts

contains all exons, e.g. *p73 α* . Values less than 100% represents the extent of expression of the isoforms with exon 11 exclusion, e.g. *p73 γ* .

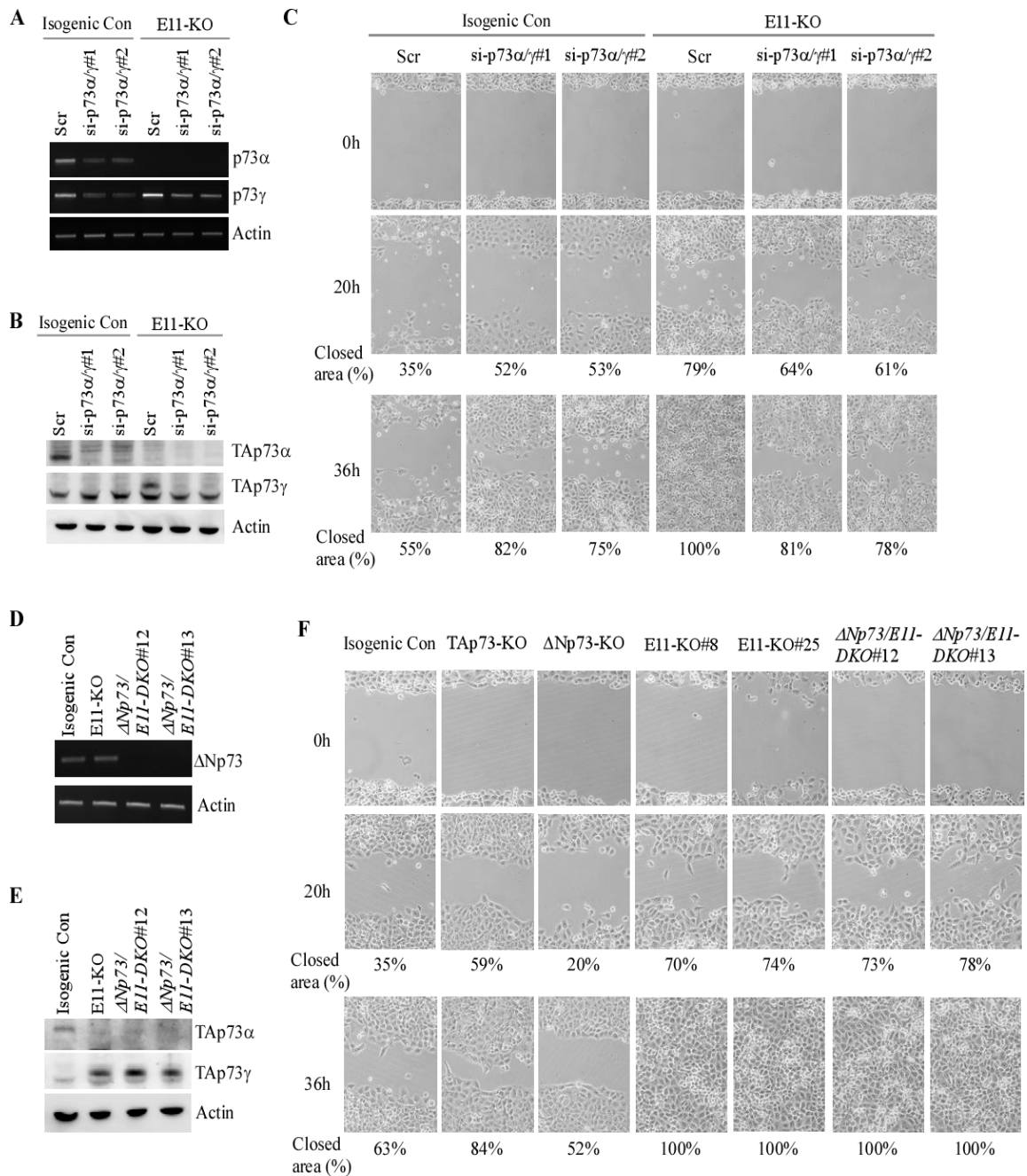
(C) The Level of *p73 α* , *p73 γ* , and actin transcript was examined in three normal dog lymph nodes and 16 dog lymphomas.

Figure 2 Deletion of Exon 11 in the *TP73* gene leads to isoform switch from α to γ , resulting in enhanced cell proliferation and migration as well as altered epithelial morphogenesis.



- (A) Schematic representation of p73 isoforms and isoform switch resulting from E11 deletion.
- (B) The level of p73 splicing variants was examined by RT-PCR in isogenic control and E11-KO H1299 cells.
- (C) The level of TAp73 α , TAp73 γ , and actin protein was measured in isogenic control and E11-KO H1299 cells mock-treated or treated with camptothecin (CPT).
- (D) The level of TAp73 α , TAp73 γ , and actin protein was measured in isogenic control, TAp73-KO, Δ Np73-KO, and E11-KO H1299 cells.
- (E) Colony formation was performed with isogenic control, TAp73-KO, Δ Np73-KO, and E11-KO H1299 cells. The was quantified as relative density.
- (F) Scratch assay was performed with isogenic control, TAp73-KO, Δ Np73-KO, and E11-KO H1299 cells. Phase contrast photomicrographs were taken immediately after scratch (0 h), 20h, and 36h later to monitor cell migration.
- (G) Representative images of parental, isogenic control, TAp73-KO, DNp73-KO, and E11-KO MCF10A cells in three-dimensional culture. Top panel: phase contrast image of acini in 3-D culture. Bottom panel: Confocal images of cross-sections through the middle of acini stained with TO-PRO-3.

Figure 3 TAp73 γ is primarily responsible for the oncogenic effects observed in E11-KO cells.



(A) Isogenic control and E11-KO H1299 cells transfected with a scrambled siRNA or siRNAs against p73 α / γ for 3 days, followed by RT-PCR analysis to measure level of p73 α , p73 γ , and actin transcripts.

(B) Cells were treated as in (A) and then subjected to western blot analysis to measure level of TAp73 α , TAp73 γ , and actin proteins using antibodies against TAp73, p73 α/γ and actin.

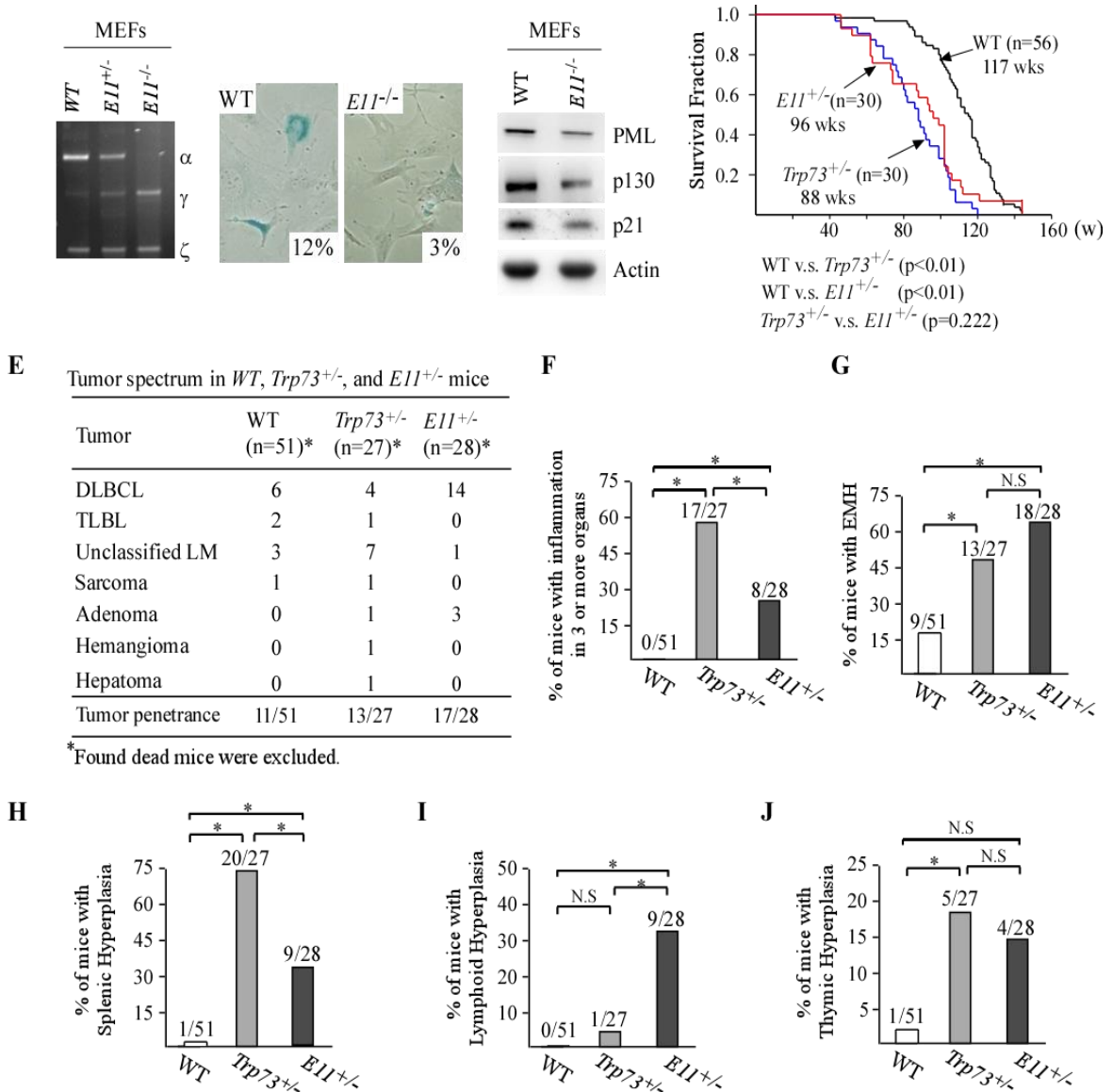
(C) Scratch assay was performed with isogenic control and E11-KO H1299 cells transfected with a scrambled siRNA or siRNAs against p73 α/γ for 3 days. Phase contrast photomicrographs were taken immediately after scratch (0 h), 20h, and 36h later to monitor cell migration.

(D) The Level of Δ Np73 and actin transcripts was measured in isogenic control, E11-KO, Δ Np73/E11-DKO H1299 cells.

(E) The Level of TAp73 α , TAp73 γ , and actin proteins was measured by western blot analysis using isogenic control, E11-KO, Δ Np73/E11-DKO H1299 cells.

(F) Scratch assay was performed with isogenic control, TAp73-KO, Δ Np73-KO, E11-KO, and Δ Np73/E11-DKO H1299 cells. Phase contrast photomicrographs were taken immediately after scratch (0 h), 20h, and 36h later to monitor cell migration.

Figure 4 Deletion of E11 in the *Trp73* gene leads to shortened lifespan, increased incidence of spontaneous tumor and chronic inflammation in mice.

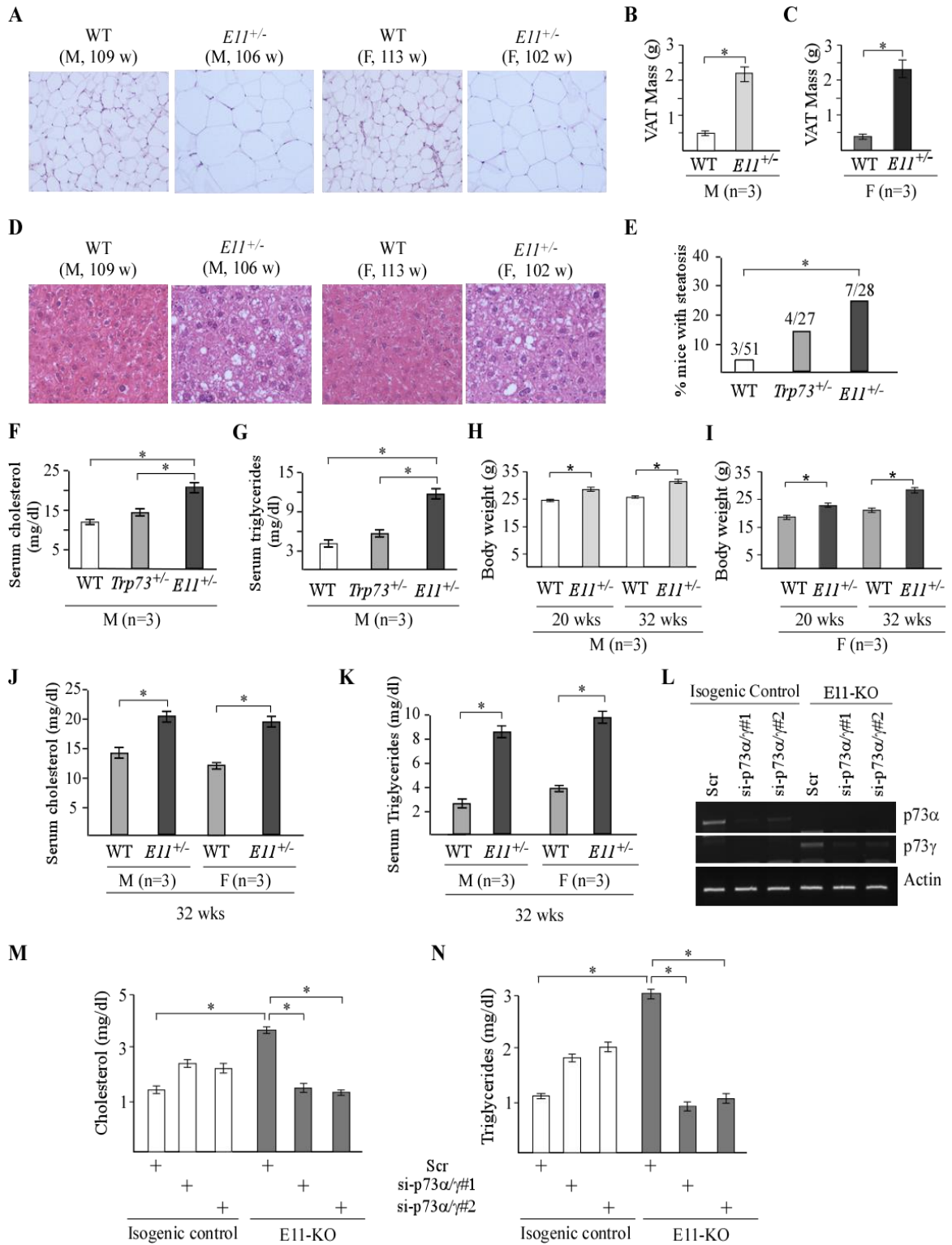


(A) The level of *Trp73* α , *Trp73* γ , *Trp73* ζ and actin transcripts were measured in WT, *E11*^{+/-}, and *E11*^{-/-} MEFs by RT-PCR analysis.

(B) SA- β -gal staining was performed with WT and *E11*^{-/-} MEFs. The percentage of SA- β -gal-positive cells was shown in each panel.

- (C) Western blot was performed to measure the level of PML, p130, p21, and actin proteins in WT and *E11*^{-/-} MEFs using antibodies against PML, p130, p21, and actin.
- (D) Kaplan-Meyer survival curves of WT (n=56), *Trp73*^{+/-} (n=30), and *E11*^{+/-} (n=30) mice.
- (E) Tumor spectra in WT (n=56), *Trp73*^{+/-} (n=27), and *E11*^{+/-} (n=28) mice.
- (F) Percentage of WT, *Trp73*^{+/-}, and *E11*^{+/-} mice with inflammation in 3 or more organs.
- (G) Percentage of WT, *Trp73*^{+/-}, and *E11*^{+/-} mice with extramedullary hematopoiesis.
- (H) Percentage of WT, *Trp73*^{+/-}, and *E11*^{+/-} mice with splenic hyperplasia.
- (I) Percentage of WT, *Trp73*^{+/-}, and *E11*^{+/-} mice with lymphoid follicular hyperplasia.
- (J) Percentage of WT, *Trp73*^{+/-}, and *E11*^{+/-} mice with thymic hyperplasia.

Figure 5 E11-deficient mice are prone to obesity.



(A) Representative images of H.E stained visceral adipose tissues from male and female WT and *E11^{+/-}* mice.

(B-C) VAT mass of male (B) and female (C) WT and *E11^{+/-}* mice at ~100 weeks.

(D) Representative images of H.E stained liver tissues from male and female WT and *E11^{+/-}* mice.

(E) Percentage of WT, *Trp73^{+/-}*, and *E11^{+/-}* mice with liver steatosis.

(F-G) The level of serum cholesterol (F) and triglycerides (G) was measured in male WT, *Trp73^{+/-}*, and *E11^{+/-}* mice at 100 weeks.

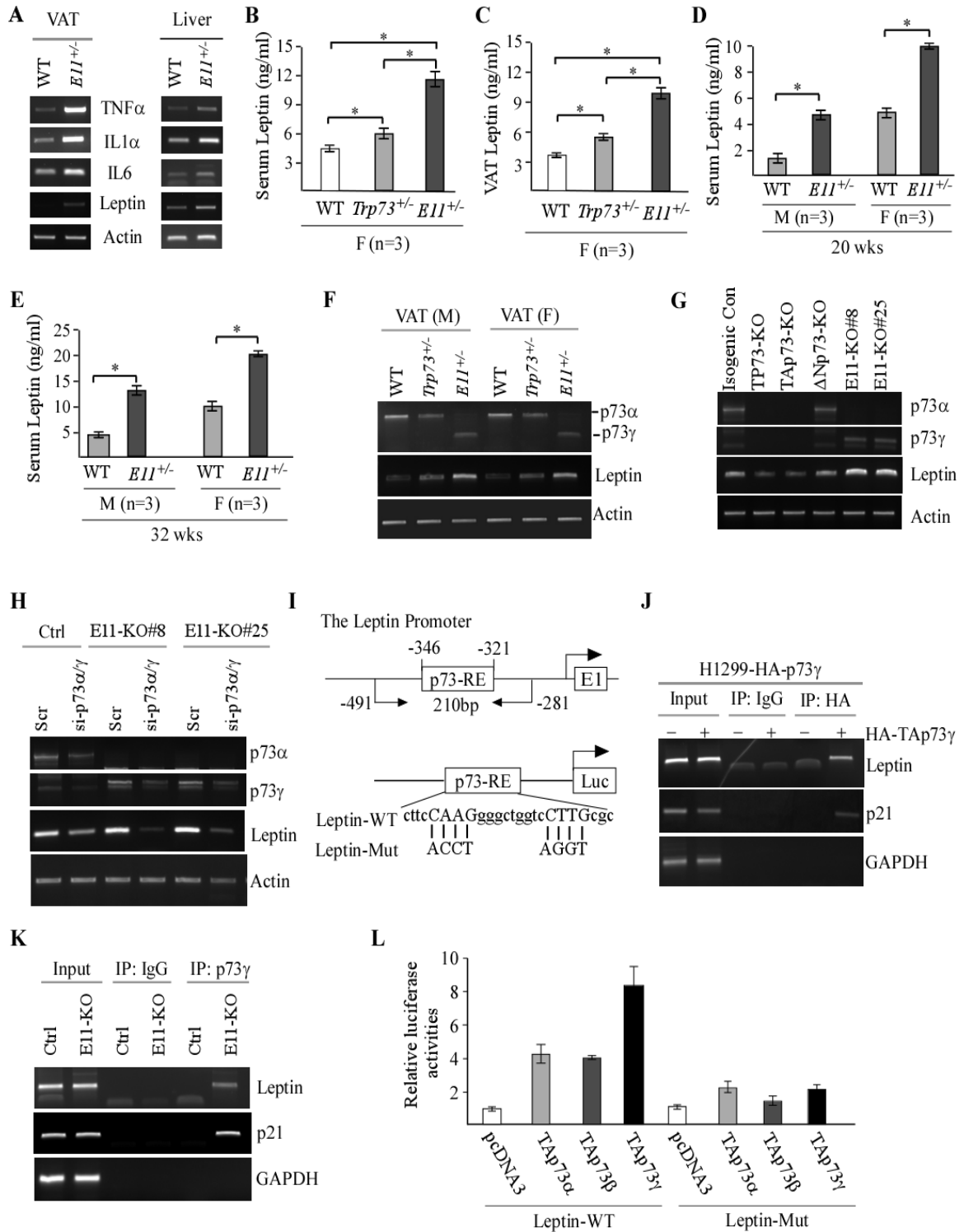
(H-I) Body weights were measured in male (H) and female (I) WT, *Trp73^{+/-}*, and *E11^{+/-}* mice at 20 or 32 weeks.

(J-K) The level of serum cholesterol (J) and triglycerides (K) was measured in male and female WT, *Trp73^{+/-}*, and *E11^{+/-}* mice at 32 weeks.

(L) The level of p73 α , p73 γ , and actin transcripts was measured in isogenic control and E11-KO H1299 cells transfected with a scrambled siRNA or siRNAs against p73 α/γ .

(M-N) Cells were treated as in (L), followed by measurement of cholesterol (M) and triglycerides (N).

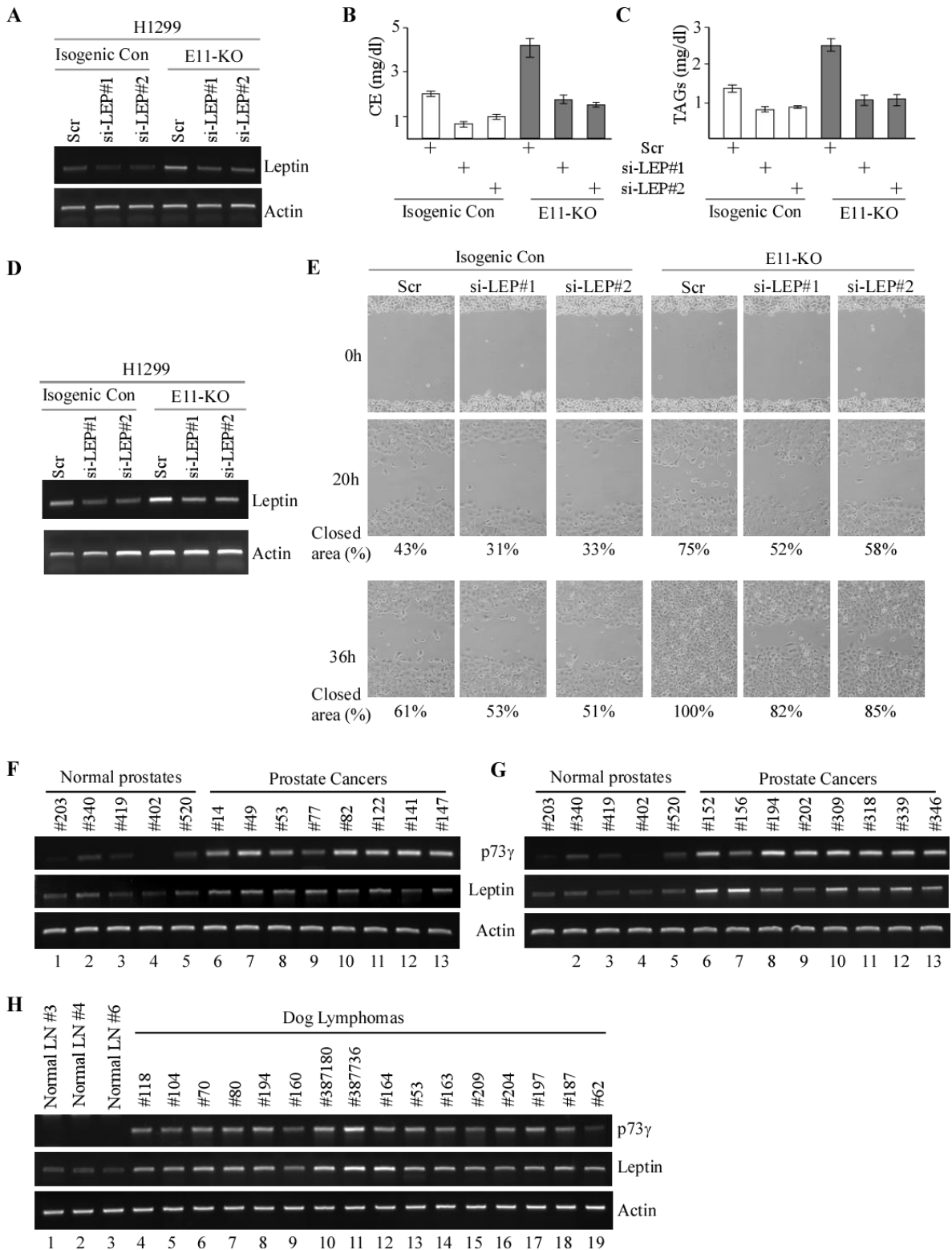
Figure 6 *E11* deficiency leads to elevated production of Leptin, a novel target of *TAp73 γ* .



(A) The level of TNF α , IL1, IL-1 α , Leptin, and actin transcripts was measured in VAT and liver from WT and *E11*^{+/-} mice.

- (B-C)** The level of serum (B) and VAT (C) Leptin was measured in female WT, *Trp73^{+/-}*, and *E11^{+/-}* mice at 65 weeks.
- (D-E)** The level of serum leptin was measured in male and female WT and *E11^{+/-}* mice at 20 (D) or 32 (E) weeks.
- (F)** The level of p73, Leptin, and actin transcripts was measured in VATs from male and female WT, *Trp73^{+/-}*, and *E11^{+/-}* mice.
- (G)** The level of p73 α , p73 γ , Leptin, and actin transcripts was measured isogenic control, total p73-KO, TAp73-KO, DNp73-KO, and E11-KO H1299 cells.
- (H)** The levels of p73 α , p73 γ , Leptin, and actin transcripts was measured isogenic control and E11-KO H1299 cells transfected with a scrambled siRNA or siRNA against for p73 α/γ for 3 days.
- (I)** Schematic representation of the Leptin promoter, the location of p73-RE as well as luciferase reporters with WT or mutant p73RE.
- (J)** H1299 cells were uninduced or induced to express TAp73 γ for 24 hours, followed by ChIP assay to measure the binding of TAp73 γ to the Leptin, p21 and GAPDH promoter.
- (K)** Isogenic control and E11-KO cells were used for ChIP assay to examine the binding of p73 γ to Leptin and p21 promoter.
- (L)** Luciferase assay was performed with H1299 cells transfected with a control vector or vector expressing TAp73 α , TAp73 β , and TAp73 γ . The relative fold-change of luciferase activity was calculated as a ratio of luciferase activity of each construct versus an empty vector.

Figure 7 Leptin is a critical mediator of TAp73 γ -mediated oncogenesis and altered lipid storage.



(A and D) The level of Leptin and actin transcripts was measured in isogenic control and E11-KO H1299 cells transfected with a scrambled siRNA or siRNAs against Leptin.

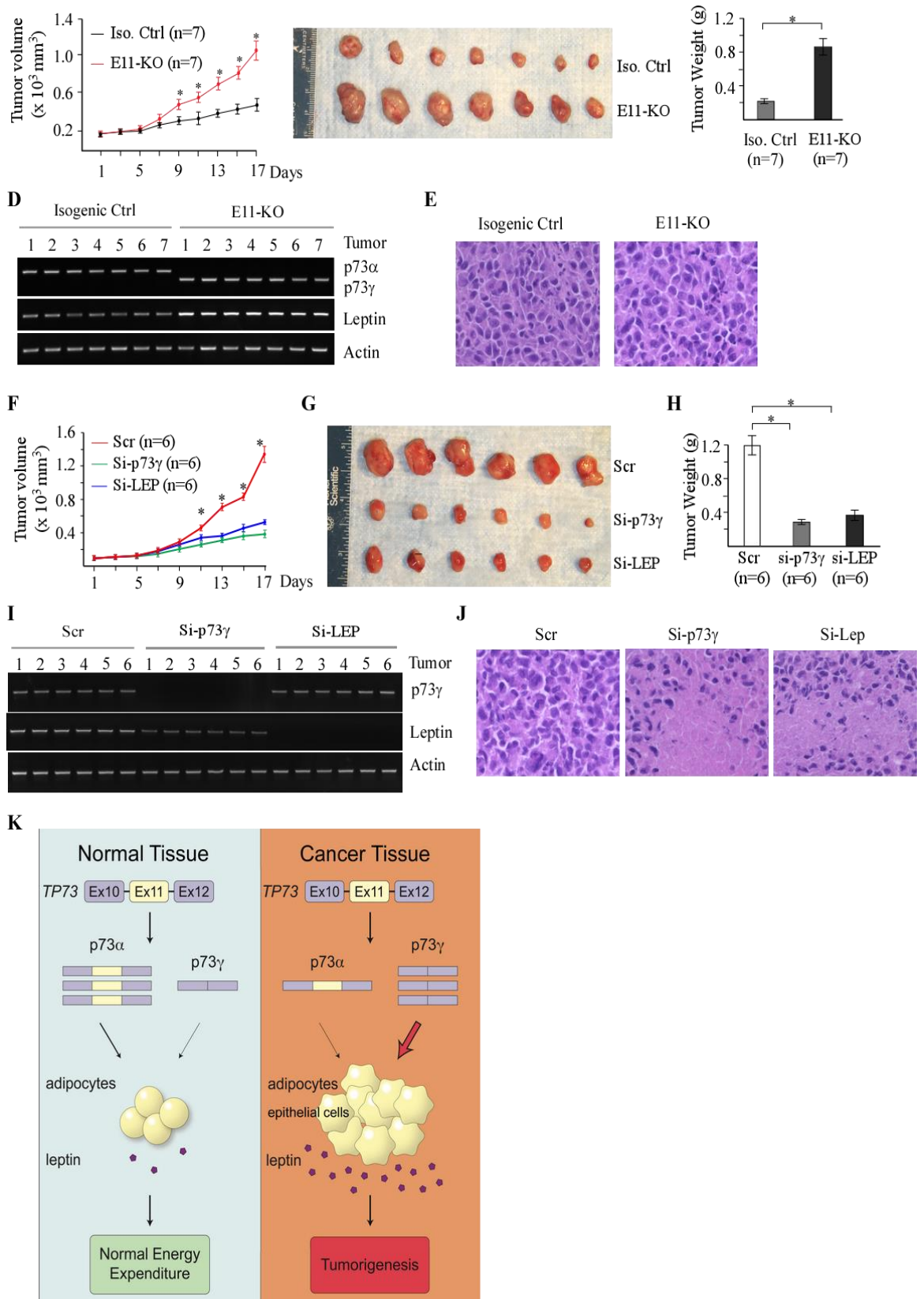
(B-C) The level of cholesterol (B) and triglycerides (C) was measured in cells treated as in (A).

(E) Scratch assay was performed with H1299 cells treated as in (D). Phase contrast photomicrographs were taken immediately after scratch (0 h), 20h, and 36h later to monitor cell migration.

(F-G) The level of p73 γ , Leptin and actin transcripts was examined in five normal prostates and 16 human prostate carcinomas.

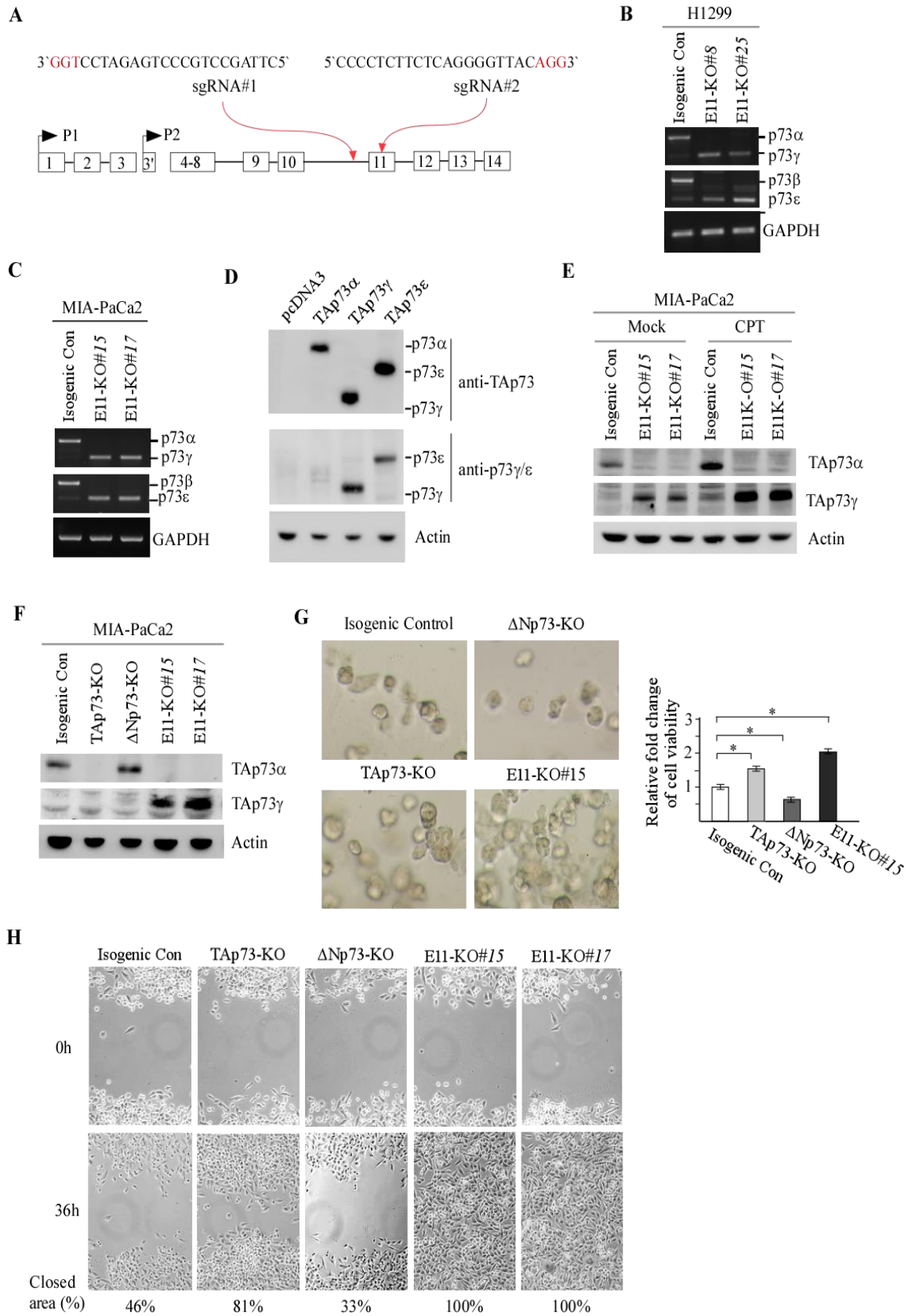
(H) The Levels of p73 γ , Leptin and actin were examined in three normal dog lymph nodes and 16 dog lymphomas.

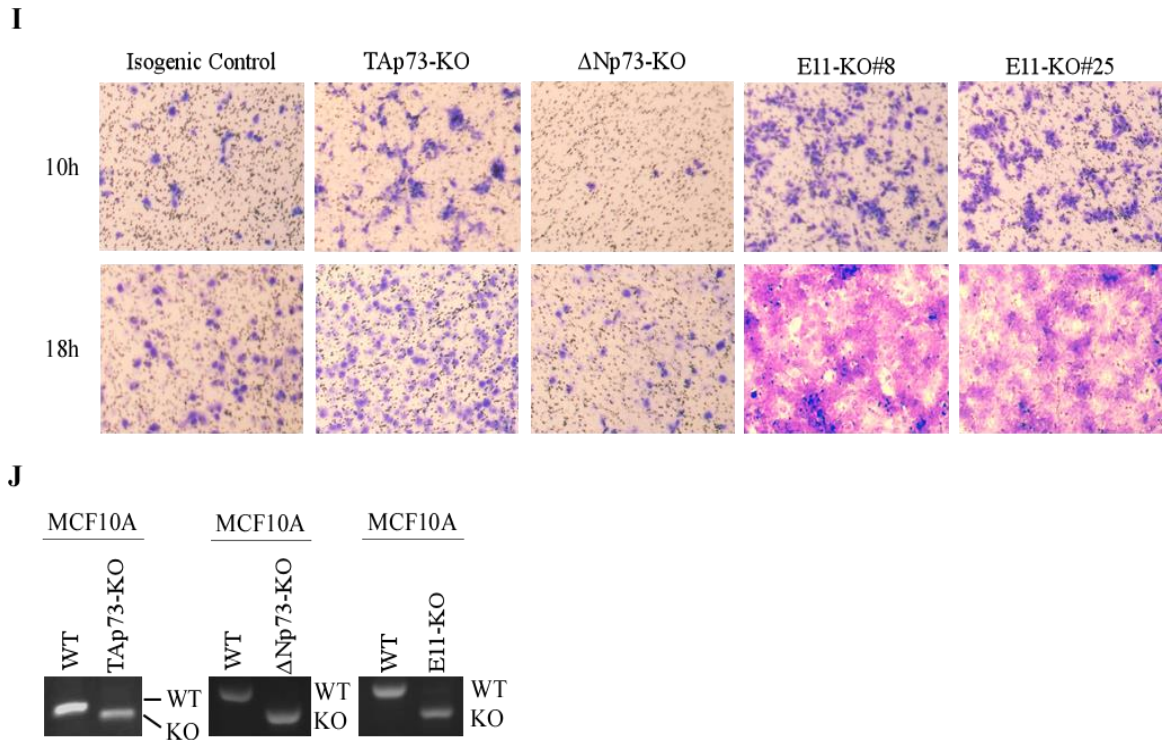
Fig. 8 Targeting p73 γ or Leptin inhibits tumor growth *in vivo*.



- (A) Xenograft tumor growth in nude mice from isogenic control or E11-KO H1299 cells (Error bars represent SEM, * indicates $p < 0.05$ by student t test).
- (B) Images of tumors excised from isogenic control and E11-KO groups.
- (C) Tumor weigh distribution between isogenic control and E11-KO groups upon termination of tumor growth experiments at day 17. (* $p < 0.05$ by Student's t-test).
- (D) The levels of p73 α , p73 γ , Leptin, and actin transcripts were measured in the tumors from isogenic control and E11-KO groups.
- (E) Representative images of H.E-stained tumors from isogenic control and E11-KO groups.
- (F) Xenograft tumor growth in nude mice from E11-KO H1299 cells transfected with scrambled siRNA or a siRNA against Leptin or p73 γ (Error bars represent SEM, * indicates $p < 0.05$ by student t test).
- (G) Images of tumors excised from E11-KO groups with or without knockdown of Leptin or p73 γ .
- (H) Tumor weigh of E11-KO tumors with or without knockdown of Leptin or p73 γ (* $p < 0.05$ by Student's t-test).
- (I) The levels of p73 α , p73 γ , Leptin, and actin transcripts were measured in E11-KO tumors with or without knockdown of Leptin or p73 γ .
- (J) Representative images of H.E-stained E11-KO tumors with or without knockdown of Leptin or p73 γ .
- (K) A proposed model to elucidate the role of p73 α/γ switch and the p73 γ -Leptin axis in tumorigenesis.

Supplemental Figure 1



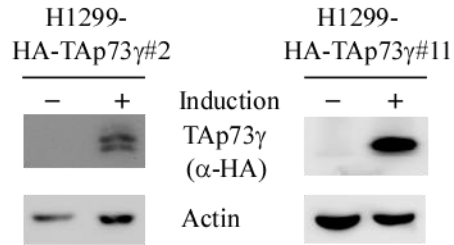


Supplemental Figure 1

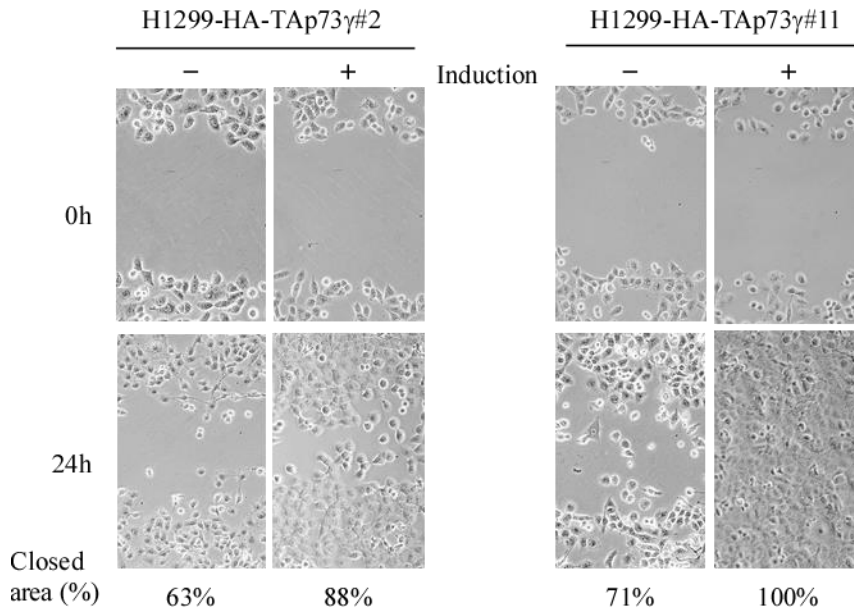
- (A) Schematic representation of the strategy to target *TP73* Exon 11 using two guide RNAs.
- (B-C) The level of p73 α/γ , p73 β/ϵ and GAPDH transcripts were measured in isogenic control and E11-KO H1299 and Mia-PaCa2 cells.
- (D) H1299 were transiently transfected with an empty pcDNA3 vector or a vector expressing HA-tagged TAp73 α , TAp73 γ , or TAp73 ϵ , followed by western blot analysis with antibodies against TAp73, p73 γ/ϵ , or actin.
- (E) The level of TAp73 α , TAp73 γ , and actin protein was measured in isogenic control and E11-KO Mia-PaCa2 cells mock-treated or treated with camptothecin (CPT).
- (F) The level of TAp73 α , TAp73 γ , and actin protein was measured in isogenic control, TAp73-KO, ΔNp73-KO, and E11-KO Mia-PaCa2 cells.
- (G) 3-D Tumor sphere assays were performed with isogenic control, TAp73-KO, ΔNp73-KO, and E11-KO. Left panel: Representative phase contrast images of tumor spheres; Right panel: the viability of tumor spheres was measured using Cell-Titer Glo assay.
- (H) Scratch assay was performed with isogenic control, TAp73-KO, ΔNp73-KO, and E11-KO Mia-PaCa2 cells. Phase contrast photomicrographs were taken immediately after scratch (0 h) and 36h later to monitor cell migration.
- (I) Isogenic control, TAp73-KO, ΔNp73-KO, and E11-KO H1299 cells were subjected to transwell migration assays, followed by phase contrast photomicrographs.
- (J) Genotyping to verify the TAp73-, ΔNp73-, and E11-KO MCF10A cells.

Supplemental Figure 2

A

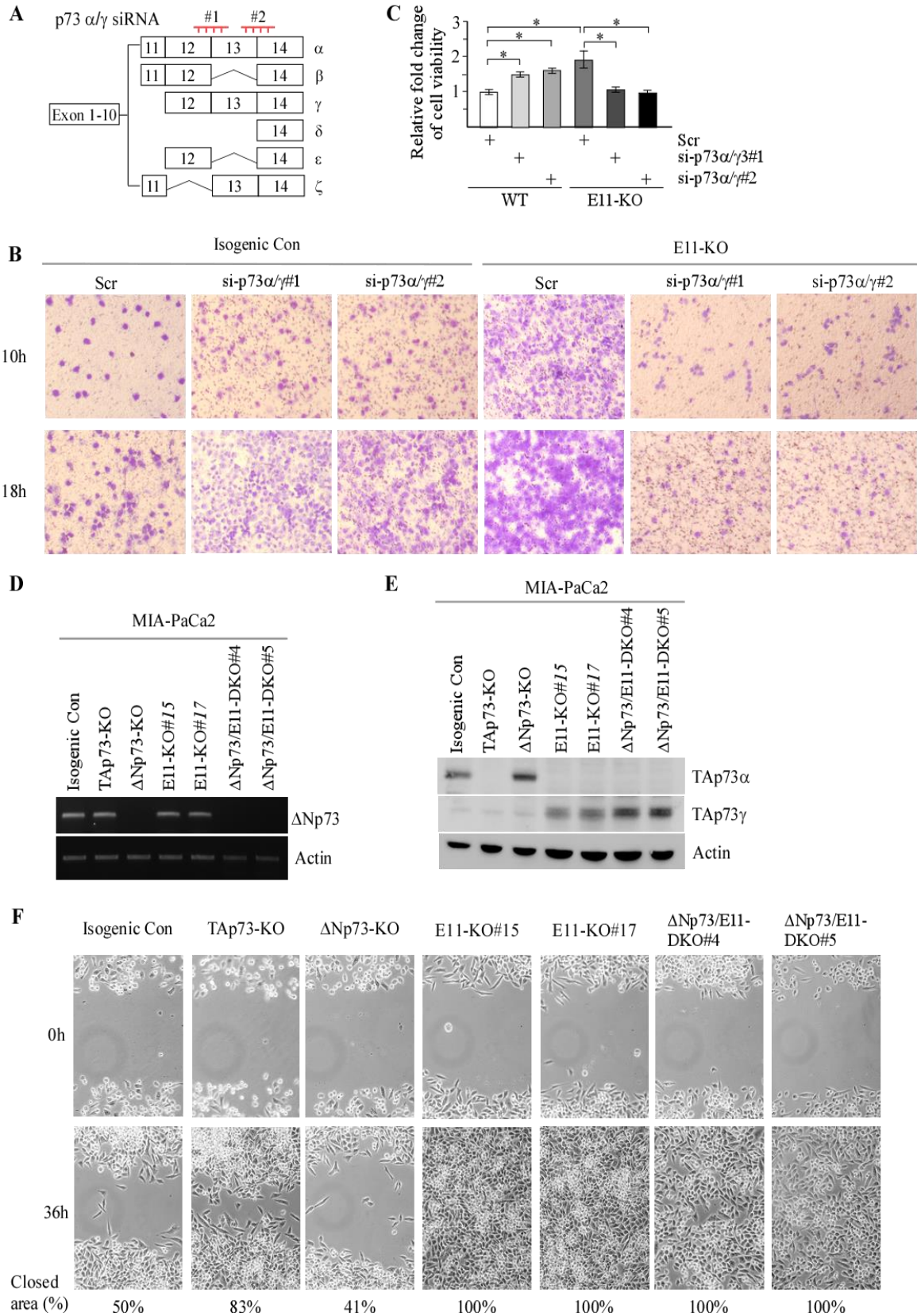


B



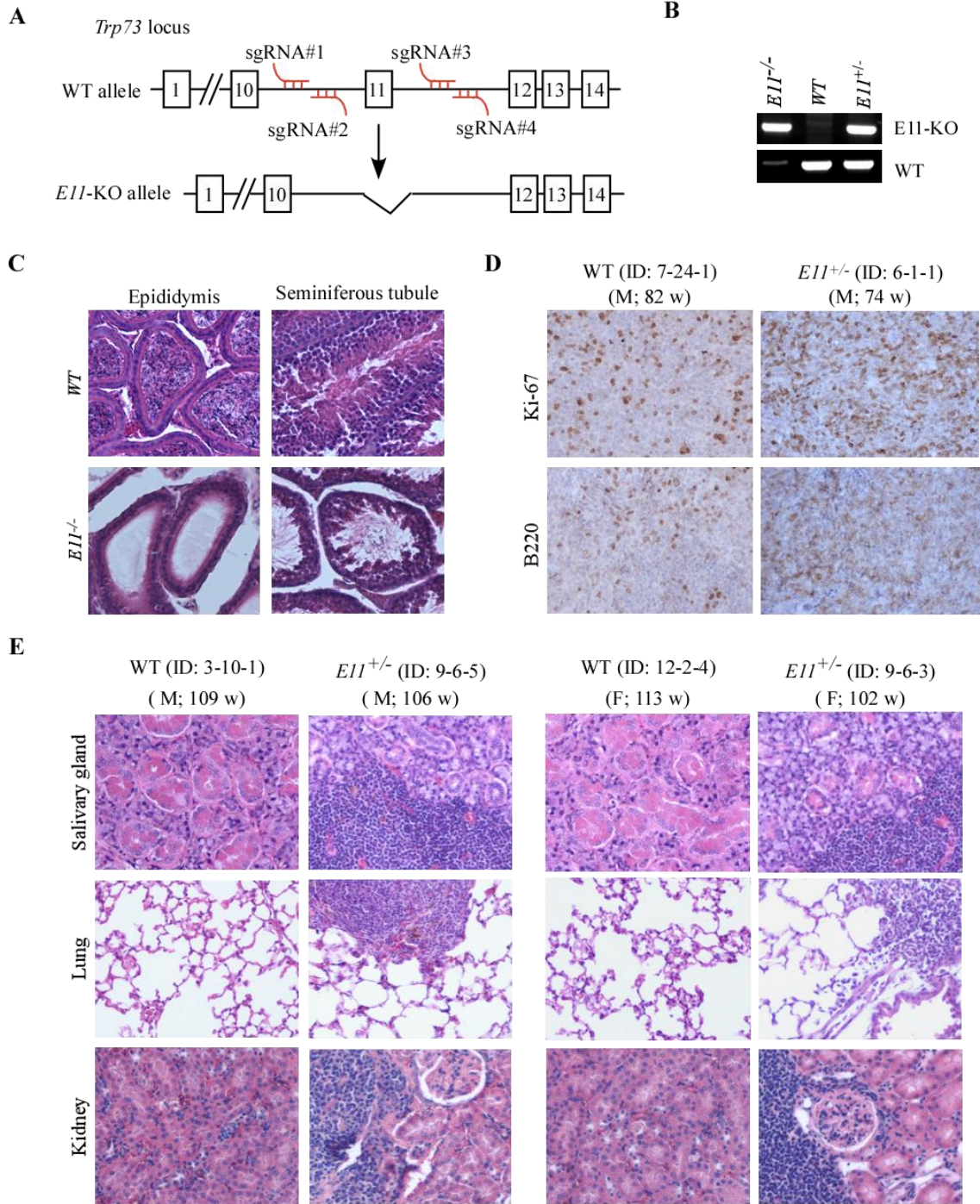
- (A) H1299 cells were uninduced or induced to express HA-tagged TAp73γ for 24 h, followed by western blot analysis with antibodies against HA or actin.
- (B) H1299 cells were uninduced or induced to express HA-tagged TAp73γ for 24 h, followed by scratch assay. Phase contrast photomicrographs were taken immediately after scratch (0 h) and 24h later to monitor cell migration.

Supplemental Figure 3



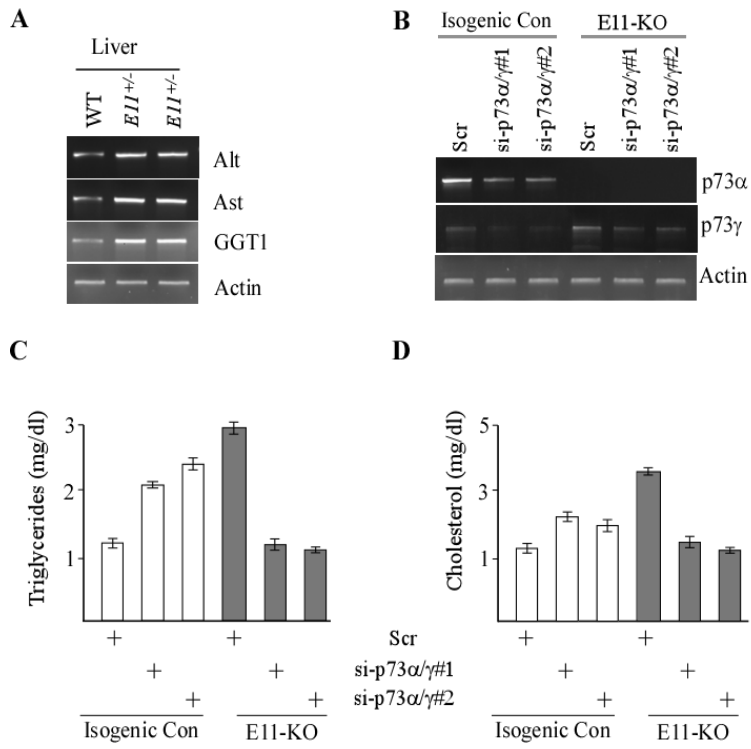
- (A) Schematic representation of the locations of p73 α/γ siRNAs.
- (B) Isogenic control and E11-KO H1299 cells were transiently transfected with a scrambled siRNA or siRNA against p73 α/γ for 3 days, followed by transwell assay. Representative images were taken by phase contrast microscope.
- (C) Isogenic control and E11-KO H1299 cells were transiently transfected with a scrambled siRNA or siRNA against p73 α/γ for 3 days, followed by measurement of 3-D tumor spheres viability.
- (D) The level of Δ Np73 and actin transcript was measured in isogenic control, TAp73-KO, Δ Np73-KO, and E11-KO, and DN/E11-DKO Mia-PaCa2 cells.
- (E) The level of TAp73 α , TAp73 γ , and actin protein was measured in isogenic control, TAp73-KO, Δ Np73-KO, E11-KO, and DN/E11-DKO Mia-PaCa2 cells.
- (F) Scratch assay was performed with isogenic control, TAp73-KO, Δ Np73-KO, E11-KO, and Δ N/E11-DKO Mia-PaCa2 cells. Phase contrast photomicrographs were taken immediately after scratch (0 h) and 36h later to monitor cell migration.

Supplemental Figure 4



- (A) Schematic representation of the strategy to generate *E11*-deficient mouse model and the location of four guide RNAs.
- (B) Genotyping to verify WT, *E11*^{+/-} and *E11*^{-/-} MEFs.
- (C) Representative images of H.E.-stained epididymis and seminiferous tubule from male WT and *E11*^{-/-} mice.
- (D) Representative images of B220- and Ki-67-stained spleen from WT and *E11*^{+/-} mice.
- (E) Representative images of H.E.-stained salivary gland, Lung, and kidney from male and female WT and *E11*^{+/-} mice.

Supplemental Figure 5

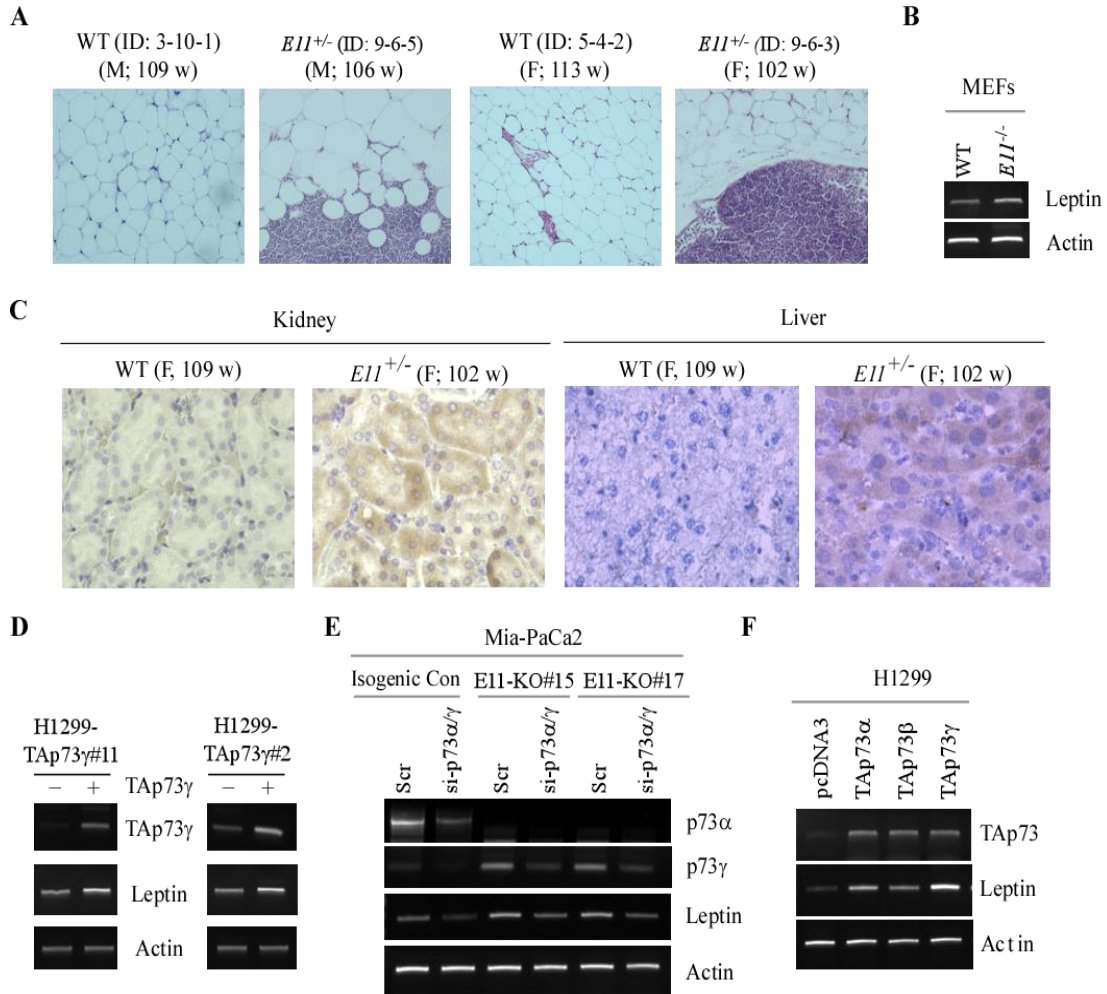


(A) The levels of Alt, Ast, and GGT1 mRNA were measured in the livers from WT and *E11*^{+/-} mice.

(B) The level of p73α, p73γ, and actin transcripts was measured in isogenic control and E11-KO Mia-PaCa2 cells transfected with a scrambled siRAN or a siRNA against p73α/γ for 3 days.

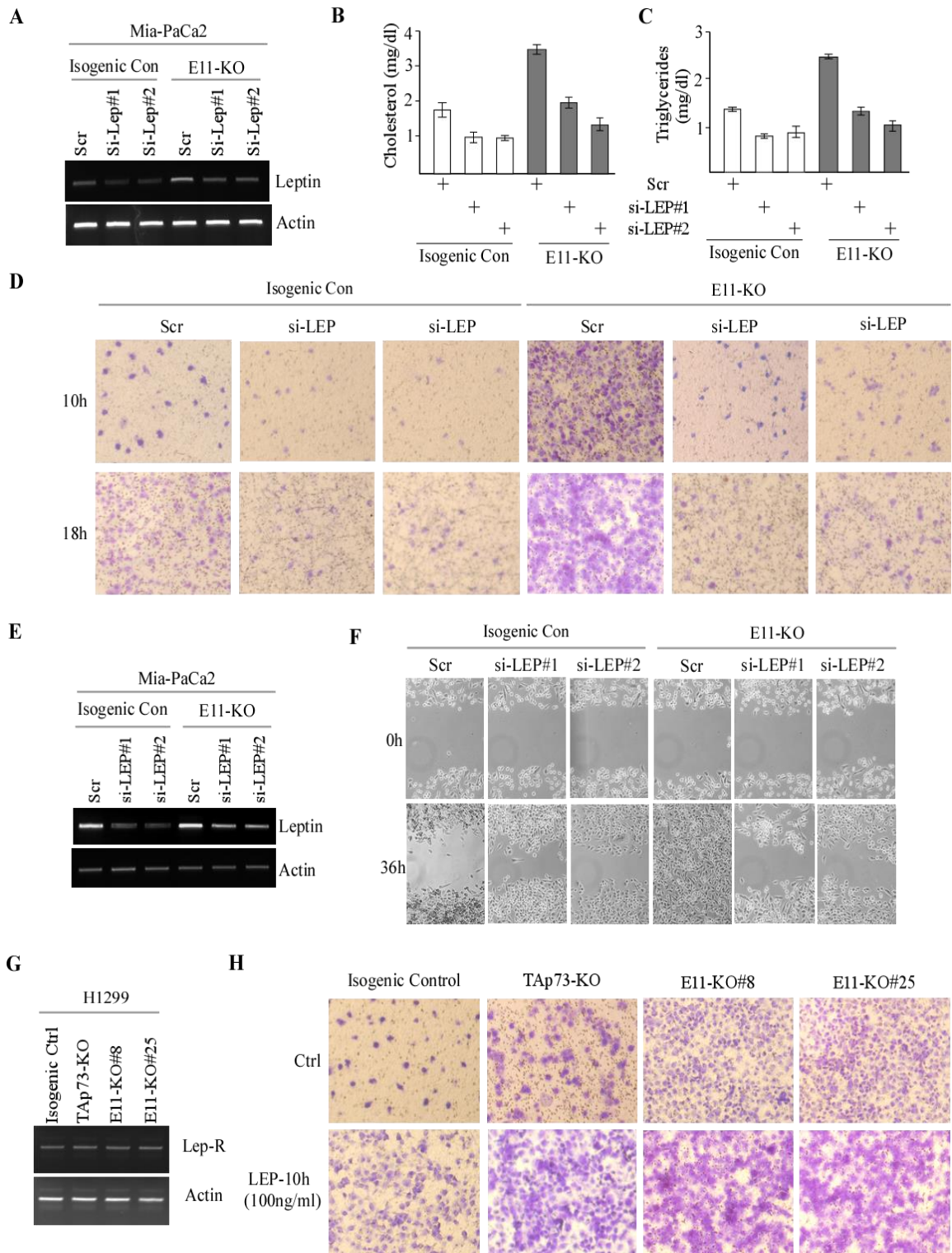
(C-D) Mia-PaCa2 cells were treated as in (A), followed by ELISA to measure the level of cholesterol (B) and triglycerides (C).

Supplemental Figure 6



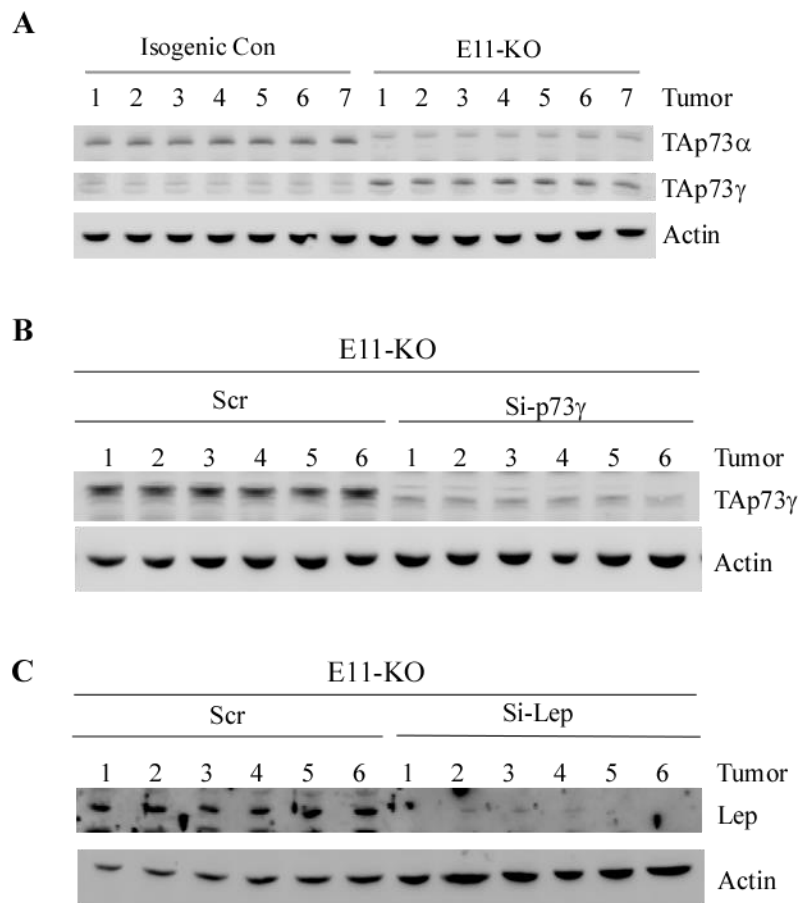
- (A) Representative images of H.E.-stained vesical adipose tissues from male and female WT and *EII*^{+/-} mice.
- (B) The level of Leptin and actin transcripts was measured in WT and *EII*^{-/-} MEFs.
- (C) Representative images of Leptin-stained livers and kidneys from WT and *EII*^{+/-} mice
- (D) H1299 cells were uninduced or induced to express HA-tagged TAp73γ for 24 hours, followed by RT-PCR analysis to measure the level of TAp73γ, Leptin, and actin transcripts.
- (E) The level of p73α, p73γ, Leptin, and actin transcripts was measured isogenic control and E11KO Mia-PaCa2 cells transfected with a scrambled siRNA or siRNA against for p73α/γ for 3 days.
- (F) The levels of TAp73, Leptin, and actin transcripts was measured in H1299 cells transiently transfected with an empty pcDNA3 vector or a pcDNA3 vector expressing TAp73α, TAp73β, or TAp73γ.

Supplemental Figure 7



- (A) The level of Leptin and actin transcripts was measured in isogenic control and E11-KO Mia-PaCa2 cells transiently transfected with a scrambled siRNA or a siRNA against Leptin for 3 days.
- (B-C) The cells were treated as in (A), followed by ELISA to measure the level of cholesterol (B) and triglycerides (C).
- (D) Isogenic control and E11-KO H1299 cells were transiently transfected with a scrambled siRNA or siRNA against Leptin for 3 days, followed by transwell assay. Representative images were taken by phase contrast microscope.
- (E) The level of Leptin and actin transcripts was measured in isogenic control and E11-KO Mia-PaCa2 cells transiently transfected with a scrambled siRNA or a siRNA against Leptin for 3 days.
- (F) The cells were treated as in (D), followed by scratch assay. Phase contrast photomicrographs were taken immediately after scratch (0 h) and 36h later to monitor cell migration.
- (G) The level of Leptin receptor and actin mRNA was examined in isogenic control, TAp73-KO, and E11-KO H1299 cells.
- (H) Transwell assay was performed with isogenic control, TAp73-KO, and E11-KO H1299 cells mocked treated or treated with 100ng/ml Leptin. Representative images were taken by phase contrast microscope.

Supplemental Figure 8



- (A) TAp73 α , TAp73 γ and actin proteins were measured in tumors from isogenic control and E11-KO groups.
- (B) TAp73 γ and actin proteins were measured in E11-KO tumors with or without p73 γ knockdown .
- (C) TAp73 γ and Leptin proteins was measured in E11-KO tumors with or without Leptin knockdown .

Supplemental Table S1: Wild-type (WT) mice (n=56) - survival time, tumor spectrum, steatosis, inflammation, and other abnormalities

ID	Gender	Survival (Wks)	Tumor	Steatosis	inflammation	Other abnormalities
5	F	134	-	-	-	-
7	F	117	-	-	-	-
16	F	100	-	-	-	-
22	F	109	-	-	-	-
25	F	109	-	-	-	-
44	F	90	-	-	-	-
55	F	104	T-LBL	-	-	-
64	F	120	-	-	-	-
2	M	127	-	-	-	-
3	M	117	-	-	Liver	-
12	M	127	-	-	-	-
13	M	127	-	-	-	-
20	M	122	-	-	-	-
23	M	122	-	-	-	-
26	M	127	-	-	Liver/Salivary gland	-
34	M	124	DLBCL	-	-	-
37	M	134	-	-	-	-
62	M	128	-	-	-	-
45	M	133	-	-	-	-
49	M	117	-	-	-	-
50	M	113	T-LBL/ DLBCL	-	-	-
56	M	117	DLBCL	-	-	-
59	M	119	DLBCL	-	-	-
65	M	106	-	-	-	-
69	M	102	DLBCL	-	-	SH
70	M	103	-	-	-	TH
71	M	90	-	-	-	-
1-24-2	M	83	-	Y	-	-
2-15-2	F	140	Lymphoma	-	-	EMH in liver
2-19-6	M	132	-	-	Pancreas	EMH in Spleen
2-19-2	F	143	-	-	-	EMH in Spleen
3-11-3	M	129	-	-	-	-
3-28-5	F	85	-	Y	-	EMH in spleen
3-9-7	M	129	-	-	-	-
5-12-3	F	99	Lymphoma	-	-	EMH in Spleen
7-9-9	F	116	-	-	-	-
8-2-6	M	120	-	-	-	-
10-24-7	F	130	-	-	Pancreas	EMH in spleen
10-26-6	F	129	Histiocytic sarcoma	-	-	EMH in spleen/liver
11-10-7	M	121	-	-	-	-
11-7-3	F	121	-	-	-	-
11-29-2	F	144	-	Y	-	EMH in spleen
12-2-4	F	113	-	-	-	-
12-20-7	F	115	-	-	-	EMH in Spleen
11-9-6	F	96	DLBCL	-	Skin	-
1-19-1	F	86	-	-	Skin	-
11-10-15	F	105	-	-	Skin/Pancreas	-
12-25-6	M	111	-	-	-	Hepatocirrhosis
1-19-5	F	109	Lymphoma	-	-	-
7-22-4	M	86	-	-	-	-
7-22-7	M	126	-	-	Kidney	-
11	M	111	N/A	-	-	Found dead
42	M	111	N/A	-	-	Found dead
43	M	107	N/A	-	-	Found dead
46	M	117	N/A	-	-	Found dead
52	M	101	N/A	-	-	Found dead

These mice were from published studies (Yang et al, 2017, PNAS, 114 (43) 11500-11505; Zhang et al, 2017, Genes & Dev, 31:1243-56)
DLBCL: Diffuse Large B-cell Lymphoma; EMH: Extramedullary Hematopoiesis; TH: Thymic Hyperplasia; SH: Splenic Hyperplasia
N/A: not applicable

Supplemental Table S2: *Trp73^{+/±}* mice (n=30) - survival time, tumor spectrum, steatosis, inflammation, and other abnormalities

ID#	Gender	Survival (Wks)	Tumor	Steatosis	Inflammation	Other abnormalities
1-30-11	F	82	-	-	Liver/Salivary gland/ kidney/ pancreas	SH/ EMH
6-7-14	M	43	-	-	Liver/lung/Kidney/ Salivary gland/skin	SH / EMH / TH
9-23-1	F	77	Hepatoma	-	Liver/pancreas/kidney	SH
12-14-3	F	46	-	-	Skin/lung/kidny/liver/salivary gland	SH / EMH
5-27-14	M	65	-	-	Liver/salivary gland	SH / EMH
9-13-11	F	69	-	-	Liver/Salivary gland/lung/kidney	SH / EMH
11-6-1	F	55	T-LBL	-	Liver/Kidney/Salivary gland/pancreas/lung	SH / EMH
5-3-5	F	105	-	Y	kidney/liver/pancreas/salivary gland	SH / EMH / TH
11-6-5	F	88	DLBCL/Hemangioma	Y	Liver/Salivary gland	SH / EMH / TH
5-13-2	M	117	-	Y	Liver/Salivary gland/Kidney	SH / EMH / TH
11-13-1/5	M	99	-	-	Liver, Salivary gland	-
10-13-12	F	89	Lymphoma	-	-	-
11-5-7	F	102	DLBCL/Lymphoma	-	Kidney/Liver/Cecum	SH
6-11-6	M	108	Lymphoma	-	Liver	SH
10-3-11	F	99	-	-	Liver/salivary gland/lung	SH / TH
10-22-4	F	86	Histiocytic sarcoma	-	Kidney/Salivary gland	-
5-28-16	F	120	Lymphoma	-	-	-
11-13-4	F	74	Lymphoma	-	-	-
12-14-1	F	103	-	-	Liver/pancreas/Salivary gland	SH
1-25-4	F	94	DLBCL	-	-	-
1-15-8	F	69	-	-	Liver/Kidney/salivary gland	SH
10-31-4	F	88	Lymphoma	-	Liver/Kidney/Lung/Salivary gland	SH/EMH
11-6-4	F	62	Gastric Adenoma	-	Lung/Salivary gland/Liver/Kidney	SH/ EMH
9-16-5	F	76	-	-	Kidney/Liver/Salivary gland	SH/EMH Liver multifocal necrosis
6-22-4	F	80	-	-	Kidney/Lung/liver	SH/EMH Liver multifocal necrosis
4-19-1	F	102	-	-	Liver/Heart	SH/LH
10-31-5	F	99	DLBCL	Y	Kidney/Lung/Salivary gland	-
10-9-2	M	101	N/A			Found dead
2-10-3	M	57	N/A			Found dead
3-10-3	M	108	N/A			Found dead

The data of the first 25 mice were from published studies (PNAS, 2019;116(48):24259-24267; J Pathol 2020; 251:284–296)
DLBCL: Diffuse Large B-cell Lymphoma; EMH: Extramedullary Hematopoiesis; SH: Splenic Hyperplasia; TH: Thymic hyperplasia;
LH: Lymphoid Hyperplasia

Supplementary table 3: *E11*^{+/-} mice (n=30) - Survival time, tumor spectrum, steatosis, inflammation, and other abnormalities

ID#	Gender	Survival (Wks)	Tumor	Steatosis	Inflammation	Other abnormalities
30	M	62	DLBCL	-	-	EMH/FPCH
16	M	46	DLBCL	-	Liver	EMH/FPCH
29	M	62	DLBCL	-	-	EMH/FPCH
11-16-15	M	46	DLBCL	-	-	-
8	F	102	DLBCL	-	kidney	-
17	F	102	MALT Lymphoma	-	-	-
6-1-2	M	74	-	-	-	LH
6-1-1	M	74	DLBCL	Y	Lung	LH
10-26-5	F	43	-	Y	Pancreas	LH/TH
3	M	88	-	Y	Kidney/Lung/Liver	LH/TH
9	M	102	Adenocarcinoma	-	Liver/Salivary gland	SH
3-6-2	F	62	-	Y	Kidney/Lung/ pancreas/ salivary gland	SH/EMH/TH/LH
7-10-8	F	94	DLBCL	-	-	EMH
7-24-7	F	73	-	-	Liver/ kidney/ pancreas/Lung/ Salivary gland	SH/EMH/LH
19	F	63	-	Y	Lung/Salivary gland	SH/EMH
6-23-4	M	52	-	-	Liver/ kidney/ pancreas/ Salivary gland	SH/EMH
7-24-3	F	102	DLBCL	-	-	-
11-18-4	M	87	-	-	GI/Lung/ pancreas/salivary gland	SH/EMH/TH
10-26-7	F	93	DLBCL	-	kidney	EMH/LH
9-6-3	F	102	-	-	Lung/salivary gland	-
7-10-5	F	111	DLBCL	-	Liver/salivary gland	EMH
9-6-4	F	104	DLBCL	-	Liver/ pancreas	EMH
9-6-5	M	106	-	Y	Kidney/Lung/ pancreas/ Salivary gland/Liver	SH/EMH/LH
11-18-6	M	96	Papillary Adenocarcinoma	Y	kidney/pancreas/salivary gland	SH/EMH/LH
10-26-1	M	99	-	-	kidney/Salivary gland/Liver	SH/EMH
9-6-10	F	112	DLBCL	-	-	EMH
7-10-2	M	144	DLBCL/Papillary Adenocarcinoma	-	kidney/Salivary gland	EMH
7-10-12	M	144	DLBCL	-	kidney	EMH
23	F	102	N/A			Found dead
7-21-4	F	121	N/A			Found dead

DLBCL: Diffuse Large B-cell Lymphoma; EMH: Extramedullary Hematopoiesis; SH: Splenic Hyperplasia; TH: Thymic Hyperplasia; LH: Lymphoid Hyperplasia; FPCH: Flord Plasma Cell Hyperplasia;

Table S4. The primers used to generate plasmids expression vectors

Name	Oligonucleotides	Sequecne
TAp73-sgRNA-1	Sense	5'-ACCGCTCCCCACGCCGGCCTCCG-3'
	Antisense	5'-AAACCGGAGGCCGGCGTGGGGAAGC-3'
TAp73-sgRNA-2	Sense	5'-CACCGTCAAACGTGGTGCCCCCATC-3'
	Antisense	5'-AAACGATGGGGGCACCACGTTTGAC-3'
Δ Np73-sgRNA-1	Sense	5'-CACCGTACAGCATGGTAGGCGCCG-3'
	Antisense	5'-AAACCGGCGCCTACCATGCTGTAC-3'
Δ Np73-sgRNA-2	Sense	5'-CACCGCGTCACACCTACCGTGGCG-3'
	Antisense	5'-AAACCGCCACGGTAGGTGTGACGC-3'
Total p73-sgRNA	Sense	5'-CACCGCACCTTCGACACCATGTCGC-3'
	Antisense	5'-AAACGCGACATGGTGTGCGAAGGTGC-3'
p73-E11-gRNA-1	Sense	5'-CACCGTCAGAAGCAACGGCTCGCAT-3'
	Antisense	5'-AAACATGCGAGCCGTTGCTTCTGAC-3'
p73-E11-gRNA-2	Sense	5'-CACCGACAGCCCCCGTCCTACGGGC-3'
	Antisense	5'-AAACGCCCCGTAGGACGGGGGCTGTC-3'
WT Leptin promoter	Forward	5'- CCC CCC GGG TCG CTG GAC CTT AGA TTC CTC ATC C -3'
	Reverse	5'- CCC AAG CTT CTT GCA ACC GCT GGC GCT G3'
Mut Leptin promoter	Forward	5'- CCC CCC GGG TCG CTG GAC CTT AGA TTC CTC ATC C -3'
	Reverse	5'- CTT CCA CCT GGG CTG GTC AGG TCG CCA -3'
TAp73 γ	Forward	5'- GAA TTC GTG GGG AGG GAA TTC ACC -3'
	Reverse	5'- CTC GAG TCA ATG GTC AGG TTC TGC AG -3'

Table S5. The primers used for genotyping mouse strains and cell lines

Name	Oligonucleotides	Sequecne
<i>P73-KO</i> mouse genotyping	Sense 1	5'- CATGTCTGGATCCGGAATAACTAACT -3'
	Sense 2	5'- CACGAGCTTGGAAGGGACTT -3'
	Antisense	5`- TC TTTAGGTGGCCTTTGAGG -3`
<i>E11-KO</i> mouse genotyping	Sense	5`- CCGAGATCACAAACAGGATG -3`
	Antisense	5`- CTACAGCTGCCTCTCAATG -3`
<i>E11-KO</i> cell line genotyping	Sense	5`- TCCACCCATTCGCAGCATG -3`
	Antisense	5`- CACTGCCCAAGGGACTCAC -3`
<i>ΔNp73-KO</i> cell line genotyping	Sense	5`- ACTAGCTGCGGAGCCTCTC -3`
	Antisense	5`- GCGTCACACCTACCGTGG -3`
<i>TAp73-KO</i> cell line genotyping	Sense	5`- GAGGCTGTCACAGGAGGAC -3`
	Antisense	5`- TCTGGCCAGCCAAGCGCAC -3`

Table S6. The primers used for RT-PCR and CHIP

Name	Oligonucleotides	Sequecne	Fragment
<i>TP73</i> (human)	Sense	5'- CAGACAGCACCTACTTTCGAC -3'	255bp
	Antisense	5'- CTGCTCATCTGGTCCATGG -3'	
LEP (human)	Sense	5'- TCACACACGCAGTCAGTCTC -3'	177bp
	Antisense	5'- GAGGTTCTCCAGGTCGTTGG -3'	
p73 α / γ (human)	Sense	5'- CAGCAGCAGCAGCTCCTACA -3'	207/356bp
	Antisense	5'- GAAATACTCGATGCAGTTTG -3'	
<i>TP73</i> -All (human)	Sense	5'- CAGCAGCAGCAGCTCCTACA -3'	94~440bp
	Antisense	5'- TACTGCTCGGGGATCTTCAG -3'	
$\Delta Np73$ (human)	Sense	5'- GATCCATGCCTCGTCCCAC -3'	155bp
	Antisense	5'- CTGCTCATCTGGTCCATGG -3'	
GAPDH (human)	Sense	5'- AGCCTCAAGATCATCAGCAATG -3'	198bp
	Antisense	5'- ATGGACTGTGTCATGAGTCCTT -3'	
<i>TP73</i> (mouse)	Sense	5'- AAGGGACTAGCGAGGCATCA -3'	232bp
	Antisense	5'- CCGGGGTAGTCGGTATTGGA -3'	
Il6 (mouse)	Sense	5'- GAGGATACCACTCCCAACAGACC -3'	284bp
	Antisense	5'- AAGTGCATCATCGTTGTTTCATACA -3'	
Lep (mouse)	Sense	5'- GGTCACTGGCTTGGACTTCA -3'	163bp
	Antisense	5'- CAGATGGAGGAGGTCTCGGA -3'	
TNF α (mouse)	Sense	5'- TGGCCTCCCTCTCATCAGTT -3'	165bp
	Antisense	5'- ACAAGGTACAACCCATCGGC -3'	
IL1a (mouse)	Sense	5'- CTCTAGAGCTCCATGCTACAGAC -3'	267bp
	Antisense	5'- TGGAATCCAGGGGAAACTG -3'	
p73 α / γ (mouse)	Sense	5'- GTGCCCCAGCCTTTGGTTGAC -3'	198/346bp
	Antisense	5'- GTGAACTCCTCTTTGATGGG -3'	
Actin (All)	Sense	5'- CTGAAGTACCCATCGAGCACGGCA -3'	221bp
	Antisense	5'- GGATAGCACAGCCTGGATAGCAACG -3'	
p73 α / γ (dog)	Sense	5'- GGGGCATCATGTGGAAATG -3'	192/361bp
	Antisense	5'- TCTCGCTCTCCGTGAACTC -3'	
LEP (dog)	Sense	5'- CTCCTCAAACAGAGGGTTCG -3'	243bp
	Antisense	5'- CCCAGGCTCTCAAAGGTCTC -3'	
GAPDH-chip	Sense	5'- AAAAGCGGGGAGAAAGTAGG -3'	202bp
	Antisense	5'- AAGAAGATGCGGCTGACTGT -3'	
Leptin-chip	Sense	5'- AGGGCCGTCGGGGCCGAGTCC -3'	210bp
	Antisense	5'- AAATCCTTGATGTCCCTCC -3'	
P21-chip	Sense	5'- GGAAGACCATGTGGACCTGT -3'	225bp
	Antisense	5'- GCGGTTTGGAGTGGTAGAAA -3'	
Alt (mouse)	Sense	5'- CGCGTCTTCCACTCAGTCT -3'	270bp
	Antisense	5'- ACCTGCTCCGTGAGTTAGC -3'	
Ast (mouse)	Sense	5'- CAGGGAGAATCGGGTTGGAG -3'	211bp
	Antisense	5'- CTTCTCCGCATCCCAGTAGC -3'	
Ggt1 (mouse)	Sense	5'- TCTGTTGCACTGGCCATCAT -3'	211bp
	Antisense	5'- CTCGAACGACAGCCTGAACT -3'	
LepR (human)	Sense	5'- CTGTGCCAACAGCCAAACTC -3'	198bp
	Antisense	5'- ATGGTACCAATGGTGGGCTG -3'	

References

1. Kaghad M, Bonnet H, Yang A, Creancier L, Biscan JC, Valent A, et al. Monoallelically expressed gene related to p53 at 1p36, a region frequently deleted in neuroblastoma and other human cancers. *Cell*. 1997;90(4):809-19.
2. Harms K, Nozell S, Chen X. The common and distinct target genes of the p53 family transcription factors. *Cell Mol Life Sci*. 2004;61(7-8):822-42.
3. Ichimiya S, Nakagawara A, Sakuma Y, Kimura S, Ikeda T, Satoh M, et al. p73: structure and function. *Pathol Int*. 2000;50(8):589-93.
4. Ozaki T, Nakagawara A. p73, a sophisticated p53 family member in the cancer world. *Cancer Sci*. 2005;96(11):729-37.
5. Nomoto S, Haruki N, Kondo M, Konishi H, Takahashi T, Takahashi T, et al. Search for mutations and examination of allelic expression imbalance of the p73 gene at 1p36.33 in human lung cancers. *Cancer Res*. 1998;58(7):1380-3.
6. Nimura Y, Mihara M, Ichimiya S, Sakiyama S, Seki N, Ohira M, et al. p73, a gene related to p53, is not mutated in esophageal carcinomas. *Int J Cancer*. 1998;78(4):437-40.
7. Yang A, Walker N, Bronson R, Kaghad M, Oosterwegel M, Bonnin J, et al. p73-deficient mice have neurological, pheromonal and inflammatory defects but lack spontaneous tumours. *Nature*. 2000;404(6773):99-103.
8. Nemajerova A, Kramer D, Siller SS, Herr C, Shomroni O, Pena T, et al. TAp73 is a central transcriptional regulator of airway multiciliogenesis. *Genes Dev*. 2016;30(11):1300-12.
9. Marshall CB, Mays DJ, Beeler JS, Rosenbluth JM, Boyd KL, Santos Guasch GL, et al. p73 Is Required for Multiciliogenesis and Regulates the Foxj1-Associated Gene Network. *Cell Rep*. 2016;14(10):2289-300.
10. Tissir F, Ravni A, Achouri Y, Riethmacher D, Meyer G, Goffinet AM. DeltaNp73 regulates neuronal survival in vivo. *Proc Natl Acad Sci U S A*. 2009;106(39):16871-6.
11. Wilhelm MT, Rufini A, Wetzel MK, Tsuchihara K, Inoue S, Tomasini R, et al. Isoform-specific p73 knockout mice reveal a novel role for delta Np73 in the DNA damage response pathway. *Genes Dev*. 2010;24(6):549-60.
12. Tomasini R, Tsuchihara K, Wilhelm M, Fujitani M, Rufini A, Cheung CC, et al. TAp73 knockout shows genomic instability with infertility and tumor suppressor functions. *Genes Dev*. 2008;22(19):2677-91.
13. Rufini A, Niklison-Chirou MV, Inoue S, Tomasini R, Harris IS, Marino A, et al. TAp73 depletion accelerates aging through metabolic dysregulation. *Genes Dev*. 2012;26(18):2009-14.
14. Inoue S, Tomasini R, Rufini A, Elia AJ, Agostini M, Amelio I, et al. TAp73 is required for spermatogenesis and the maintenance of male fertility. *Proc Natl Acad Sci U S A*. 2014;111(5):1843-8.
15. Dulloo I, Phang BH, Othman R, Tan SY, Vijayaraghavan A, Goh LK, et al. Hypoxia-inducible TAp73 supports tumorigenesis by regulating the angiogenic transcriptome. *Nat Cell Biol*. 2015;17(4):511-23.
16. Nemajerova A, Amelio I, Gebel J, Dotsch V, Melino G, Moll UM. Non-oncogenic roles of TAp73: from multiciliogenesis to metabolism. *Cell Death Differ*. 2018;25(1):144-53.
17. Rufini A, Agostini M, Grespi F, Tomasini R, Sayan BS, Niklison-Chirou MV, et al. p73 in Cancer. *Genes Cancer*. 2011;2(4):491-502.
18. Stiewe T, Putzer BM. Role of p73 in malignancy: tumor suppressor or oncogene? *Cell Death Differ*. 2002;9(3):237-45.
19. Amelio I, Inoue S, Markert EK, Levine AJ, Knight RA, Mak TW, et al. TAp73 opposes tumor angiogenesis by promoting hypoxia-inducible factor 1alpha degradation. *Proc Natl Acad Sci U S A*. 2015;112(1):226-31.

20. Li L, Li L, Li W, Chen T, Bin Z, Zhao L, et al. TAp73-induced phosphofructokinase-1 transcription promotes the Warburg effect and enhances cell proliferation. *Nat Commun.* 2018;9(1):4683.
21. Sharif T, Dai C, Martell E, Ghassemi-Rad MS, Hanes MR, Murphy PJ, et al. TAp73 Modifies Metabolism and Positively Regulates Growth of Cancer Stem-Like Cells in a Redox-Sensitive Manner. *Clin Cancer Res.* 2019;25(6):2001-17.
22. Murray-Zmijewski F, Lane DP, Bourdon JC. p53/p63/p73 isoforms: an orchestra of isoforms to harmonise cell differentiation and response to stress. *Cell Death Differ.* 2006;13(6):962-72.
23. Vikhrev A, Melino G, Amelio I. p73 Alternative Splicing: Exploring a Biological Role for the C-Terminal Isoforms. *J Mol Biol.* 2018;430(13):1829-38.
24. Liu G, Chen X. The C-terminal sterile alpha motif and the extreme C terminus regulate the transcriptional activity of the alpha isoform of p73. *J Biol Chem.* 2005;280(20):20111-9.
25. Ueda Y, Hijikata M, Takagi S, Chiba T, Shimotohno K. New p73 variants with altered C-terminal structures have varied transcriptional activities. *Oncogene.* 1999;18(35):4993-8.
26. Ozaki T, Naka M, Takada N, Tada M, Sakiyama S, Nakagawara A. Deletion of the COOH-terminal region of p73alpha enhances both its transactivation function and DNA-binding activity but inhibits induction of apoptosis in mammalian cells. *Cancer Res.* 1999;59(23):5902-7.
27. Sabapathy K. p73: a Positive or Negative Regulator of Angiogenesis, or Both? *Mol Cell Biol.* 2015;36(6):848-54.
28. Zhang Y, Proenca R, Maffei M, Barone M, Leopold L, Friedman JM. Positional cloning of the mouse obese gene and its human homologue. *Nature.* 1994;372(6505):425-32.
29. Coleman DL. A historical perspective on leptin. *Nat Med.* 2010;16(10):1097-9.
30. Friedman JM. Leptin and the endocrine control of energy balance. *Nat Metab.* 2019;1(8):754-64.
31. Farooqi IS, Jebb SA, Langmack G, Lawrence E, Cheetham CH, Prentice AM, et al. Effects of recombinant leptin therapy in a child with congenital leptin deficiency. *New Engl J Med.* 1999;341(12):879-84.
32. Frederich RC, Hamann A, Anderson S, Lollmann B, Lowell BB, Flier JS. Leptin Levels Reflect Body Lipid-Content in Mice - Evidence for Diet-Induced Resistance to Leptin Action. *Nature Medicine.* 1995;1(12):1311-4.
33. Bennett BD, Solar GP, Yuan JQ, Mathias J, Thomas GR, Matthews W. A role for leptin and its cognate receptor in hematopoiesis. *Curr Biol.* 1996;6(9):1170-80.
34. Chehab FF, Lim ME, Lu R. Correction of the sterility defect in homozygous obese female mice by treatment with the human recombinant leptin. *Nat Genet.* 1996;12(3):318-20.
35. Ducy P, Amling M, Takeda S, Priemel M, Schilling AF, Beil FT, et al. Leptin inhibits bone formation through a hypothalamic relay: A central control of bone mass. *Cell.* 2000;100(2):197-207.
36. Sierra-Honigmann MR, Nath AK, Murakami C, Garcia-Cardena G, Papapetropoulos A, Sessa WC, et al. Biological action of leptin as an angiogenic factor. *Science.* 1998;281(5383):1683-6.
37. Ray A, Cleary MP. The potential role of leptin in tumor invasion and metastasis. *Cytokine Growth F R.* 2017;38:80-97.
38. Xu CJ, Dong LL, Kang XL, Li ZM, Zhang HY. Leptin promotes proliferation and inhibits apoptosis of prostate cancer cells by regulating ERK1/2 signaling pathway. *Eur Rev Med Pharmacol Sci.* 2020;24(16):8341-8.
39. Hosney M, Sabet S, El-Shinawi M, Gaafar KM, Mohamed MM. Leptin is overexpressed in the tumor microenvironment of obese patients with estrogen receptor positive breast cancer. *Experimental and Therapeutic Medicine.* 2017;13(5):2235-46.
40. Lin TC, Hsiao M. Leptin and Cancer: Updated Functional Roles in Carcinogenesis, Therapeutic Niches, and Developments. *Int J Mol Sci.* 2021;22(6).

41. Karabulut S, Afsar CU, Karabulut M, Alis H, Erturk K, Karaman S, et al. Serum leptin levels may have diagnostic and predictive roles in patients with pancreatic adenocarcinoma treated with gemcitabine-based chemotherapy. *Journal of Buon*. 2016;21(4):895-902.
42. Ran FA, Hsu PD, Wright J, Agarwala V, Scott DA, Zhang F. Genome engineering using the CRISPR-Cas9 system. *Nat Protoc*. 2013;8(11):2281-308.
43. Zhang J, Sun W, Kong X, Zhang Y, Yang HJ, Ren C, et al. Mutant p53 antagonizes p63/p73-mediated tumor suppression via Notch1. *Proc Natl Acad Sci U S A*. 2019;116(48):24259-67.
44. Zhang J, Cho SJ, Shu L, Yan W, Guerrero T, Kent M, et al. Translational repression of p53 by RNPC1, a p53 target overexpressed in lymphomas. *Genes Dev*. 2011;25(14):1528-43.
45. Dohn M, Nozell S, Willis A, Chen X. Tumor suppressor gene-inducible cell lines. *Methods Mol Biol*. 2003;223:221-35.
46. Yan W, Chen X. GPX2, a direct target of p63, inhibits oxidative stress-induced apoptosis in a p53-dependent manner. *J Biol Chem*. 2006;281(12):7856-62.
47. Dohn M, Zhang S, Chen X. p63alpha and DeltaNp63alpha can induce cell cycle arrest and apoptosis and differentially regulate p53 target genes. *Oncogene*. 2001;20(25):3193-205.
48. Harms KL, Chen X. The C terminus of p53 family proteins is a cell fate determinant. *Mol Cell Biol*. 2005;25(5):2014-30.
49. Suarez-Arnedo A, Torres Figueroa F, Clavijo C, Arbelaez P, Cruz JC, Munoz-Camargo C. An image J plugin for the high throughput image analysis of in vitro scratch wound healing assays. *PLoS One*. 2020;15(7):e0232565.
50. Qian Y, Zhang J, Yan B, Chen X. DEC1, a basic helix-loop-helix transcription factor and a novel target gene of the p53 family, mediates p53-dependent premature senescence. *J Biol Chem*. 2008;283(5):2896-905.
51. Zhang Y, Yan W, Chen X. Mutant p53 disrupts MCF-10A cell polarity in three-dimensional culture via epithelial-to-mesenchymal transitions. *J Biol Chem*. 2011;286(18):16218-28.
52. Justus CR, Leffler N, Ruiz-Echevarria M, Yang LV. In vitro Cell Migration and Invasion Assays. *Jove-J Vis Exp*. 2014(88).
53. Janik P, Briand P, Hartmann NR. The effect of estrone-progesterone treatment on cell proliferation kinetics of hormone-dependent GR mouse mammary tumors. *Cancer Res*. 1975;35(12):3698-704.
54. Zaika AI, Kovalev S, Marchenko ND, Moll UM. Overexpression of the wild type p73 gene in breast cancer tissues and cell lines. *Cancer Res*. 1999;59(13):3257-63.
55. Zhang J, Xu E, Chen X. TAp73 protein stability is controlled by histone deacetylase 1 via regulation of Hsp90 chaperone function. *J Biol Chem*. 2013;288(11):7727-37.
56. Zhang Y, Yan W, Jung YS, Chen X. Mammary epithelial cell polarity is regulated differentially by p73 isoforms via epithelial-to-mesenchymal transition. *J Biol Chem*. 2012;287(21):17746-53.
57. Bae WK, Hong CS, Park MR, Sun EG, Lee JH, Kang K, et al. TAp73 inhibits cell invasion and migration by directly activating KAI1 expression in colorectal carcinoma. *Cancer Lett*. 2018;415:106-16.
58. Zhang Y, Qian Y, Zhang J, Yan W, Jung YS, Chen M, et al. Ferredoxin reductase is critical for p53-dependent tumor suppression via iron regulatory protein 2. *Genes Dev*. 2017;31(12):1243-56.
59. Zhang J, Xu E, Ren C, Yan W, Zhang M, Chen M, et al. Mice deficient in Rbm38, a target of the p53 family, are susceptible to accelerated aging and spontaneous tumors. *Proc Natl Acad Sci U S A*. 2014;111(52):18637-42.
60. Malnick S, Chertin L, Neuman M. Gamma Glutamyl Transferase - An Underestimated Marker for Cardiovascular Disease and the Metabolic Syndrome. *J Pharm Pharm Sci*. 2020;23.
61. Sookoian S, Castano GO, Scian R, Gianotti TF, Dopazo H, Rohr C, et al. Serum aminotransferases in nonalcoholic fatty liver disease are a signature of liver metabolic perturbations at the amino acid and Krebs cycle level. *Am J Clin Nutr*. 2016;103(2):422-34.

62. Cao H. Adipocytokines in obesity and metabolic disease. *J Endocrinol.* 2014;220(2):T47-59.
63. Tilg H, Moschen AR. Adipocytokines: mediators linking adipose tissue, inflammation and immunity. *Nat Rev Immunol.* 2006;6(10):772-83.
64. Divella R, De Luca R, Abbate I, Naglieri E, Daniele A. Obesity and cancer: the role of adipose tissue and adipo-cytokines-induced chronic inflammation. *J Cancer.* 2016;7(15):2346-59.
65. Myers MG, Jr., Leibel RL, Seeley RJ, Schwartz MW. Obesity and leptin resistance: distinguishing cause from effect. *Trends Endocrinol Metab.* 2010;21(11):643-51.
66. Abella V, Scotece M, Conde J, Pino J, Gonzalez-Gay MA, Gomez-Reino JJ, et al. Leptin in the interplay of inflammation, metabolism and immune system disorders. *Nat Rev Rheumatol.* 2017;13(2):100-9.
67. de Candia P, Prattichizzo F, Garavelli S, Alviggi C, La Cava A, Matarese G. The pleiotropic roles of leptin in metabolism, immunity, and cancer. *J Exp Med.* 2021;218(5).
68. Kang YJ, Moon A. Roles of Leptin in Cancer Progression. *Biomol Ther.* 2010;18(4):363-74.
69. Lin TC, Hsiao M. Leptin and Cancer: Updated Functional Roles in Carcinogenesis, Therapeutic Niches, and Developments. *International Journal of Molecular Sciences.* 2021;22(6).
70. el-Deiry WS, Tokino T, Velculescu VE, Levy DB, Parsons R, Trent JM, et al. WAF1, a potential mediator of p53 tumor suppression. *Cell.* 1993;75(4):817-25.
71. Sanchez-Jimenez F, Perez-Perez A, de la Cruz-Merino L, Sanchez-Margalet V. Obesity and Breast Cancer: Role of Leptin. *Front Oncol.* 2019;9:596.
72. Sabol RA, Bowles AC, Cote A, Wise R, O'Donnell B, Matossian MD, et al. Leptin produced by obesity-altered adipose stem cells promotes metastasis but not tumorigenesis of triple-negative breast cancer in orthotopic xenograft and patient-derived xenograft models. *Breast Cancer Res.* 2019;21(1):67.
73. Park J, Scherer PE. Leptin and cancer: from cancer stem cells to metastasis. *Endocr Relat Cancer.* 2011;18(4):C25-9.
74. Stantic M, Sakil HA, Zirath H, Fang T, Sanz G, Fernandez-Woodbridge A, et al. TAp73 suppresses tumor angiogenesis through repression of proangiogenic cytokines and HIF-1alpha activity. *Proc Natl Acad Sci U S A.* 2015;112(1):220-5.
75. Dulloo I, Hooi PB, Sabapathy K. Hypoxia-induced DNp73 stabilization regulates Vegf-A expression and tumor angiogenesis similar to TAp73. *Cell Cycle.* 2015;14(22):3533-9.
76. Fernandez-Alonso R, Martin-Lopez M, Gonzalez-Cano L, Garcia S, Castrillo F, Diez-Prieto I, et al. p73 is required for endothelial cell differentiation, migration and the formation of vascular networks regulating VEGF and TGFbeta signaling. *Cell Death Differ.* 2015;22(8):1287-99.
77. Nozell S, Wu Y, McNaughton K, Liu G, Willis A, Paik JC, et al. Characterization of p73 functional domains necessary for transactivation and growth suppression. *Oncogene.* 2003;22(28):4333-47.
78. Chi SW, Ayed A, Arrowsmith CH. Solution structure of a conserved C-terminal domain of p73 with structural homology to the SAM domain. *EMBO J.* 1999;18(16):4438-45.
79. Nemajerova A, Petrenko O, Trumper L, Palacios G, Moll UM. Loss of p73 promotes dissemination of Myc-induced B cell lymphomas in mice. *J Clin Invest.* 2010;120(6):2070-80.
80. Tschan MP, Grob TJ, Peters UR, Laurenzi VD, Huegli B, Kreuzer KA, et al. Enhanced p73 expression during differentiation and complex p73 isoforms in myeloid leukemia. *Biochem Biophys Res Commun.* 2000;277(1):62-5.
81. Alexandrova EM, Moll UM. Role of p53 family members p73 and p63 in human hematological malignancies. *Leuk Lymphoma.* 2012;53(11):2116-29.
82. Pluta A, Nyman U, Joseph B, Robak T, Zhivotovsky B, Smolewski P. The role of p73 in hematological malignancies. *Leukemia.* 2006;20(5):757-66.
83. Friedman JM. A tale of two hormones. *Nat Med.* 2010;16(10):1100-6.

84. Considine RV, Sinha MK, Heiman ML, Kriauciunas A, Stephens TW, Nyce MR, et al. Serum immunoreactive-leptin concentrations in normal-weight and obese humans. *N Engl J Med.* 1996;334(5):292-5.
85. Considine RV, Caro JF. Leptin: genes, concepts and clinical perspective. *Horm Res.* 1996;46(6):249-56.
86. El-Haschimi K, Pierroz DD, Hileman SM, Bjorbaek C, Flier JS. Two defects contribute to hypothalamic leptin resistance in mice with diet-induced obesity. *J Clin Invest.* 2000;105(12):1827-32.
87. Pelleymounter MA, Cullen MJ, Baker MB, Hecht R, Winters D, Boone T, et al. Effects of the obese gene product on body weight regulation in ob/ob mice. *Science.* 1995;269(5223):540-3.
88. Dutta D, Ghosh S, Pandit K, Mukhopadhyay P, Chowdhury S. Leptin and cancer: Pathogenesis and modulation. *Indian J Endocrinol Metab.* 2012;16(Suppl 3):S596-600.